THESIS

HOST DIRECTED THERAPY TARGETING M.TUBERCULOSIS INFECTED MACROPHAGES

Submitted by

Natalie Lakey

Department of Microbiology, Immunology and Pathology

In partial fulfillment of the requirements

For the Degree of Master of Science

Colorado State University

Fort Collins, Colorado

Summer 2016

Master's Committee:

Advisor: Randall Basaraba

Brendan Podell
Rushika Perera
Adam Chicco

ABSTRACT

HOST DIRECTED THERAPY TARGETING M.TUBERCULOSIS INFECTED MACROPHAGES

With the rise of drug resistant strains of *Mycobacterium tuberculosis* (Mtb) and lags in antimicrobial drug development, it is imperative to explore alternative methods of treatment through host-directed adjunct therapies. Hallmarks of Mtb infection are altered host cell glucose metabolism and non-diabetic hyperglycemia, which increase disease severity and bacterial burden. This can be targeted using a combination of metformin and 2-deoxyglucose (2DG) to lower systemic blood glucose and increase metabolic stress in infected macrophages to induce apoptotic cell death, enabling Mtb clearance and antigen presentation to activate cell-mediated immune responses. We hypothesized that bacterial survival is aided by glycolysis-dependent macrophages, which can be targeted using a combination of metformin and 2DG to strengthen host immune responses. Using an *in vitro* model of guinea pig bone marrow derived macrophages under normal and high glucose conditions, we determined that both basal respiration and glycolytic activity increased after infection. When singly treated, metformin inhibited basal respiration while increasing glycolysis while 2DG inhibited both processes. In combination metformin and 2DG treatment inhibited basal respiration more effectively than metformin treatment alone and inhibited glycolysis as effectively as 2DG by itself. Efficacy of metformin-2DG treatment is dependent on high cellular glycolytic activity, a characteristic of granulomatous cells. Metformin-2DG treatment decreased cell survival 48 hours post-treatment by increasing apoptotic cell death and decreased Mtb survival more effectively than metformin or 2DG alone. We conclude that apoptotic induction of macrophages by metformin-2DG treatment may be a viable adjunct treatment to antimicrobial drugs to reduce bacterial burden and increase an effective host adaptive immune response.

TABLE OF CONTENTS

INTRODUCTION AND LITERATURE REVIEW

I. Tuberculosis

Tuberculosis is a widespread, potentially fatal infectious disease affecting the lungs and other organs of the body. In the year 2014 alone, there were 9.6 million new tuberculosis (TB) cases and 1.5 million TB-related deaths, outranking HIV as the number one cause of death due to an infectious disease worldwide[1]. While only 12% of immune-competent individuals may develop active disease, the remaining 88% of individuals who develop an asymptomatic, latent infection are still at risk of developing active disease if left untreated[2].

Mycobacterium tuberculosis (Mtb), the causative agent of TB, has developed to coexist among and within us, with the oldest confirmed case having occurred over 9,000 years ago[3]. Today, Mtb continues to evolve to maintain this coexistence even in the presence of antimicrobial therapies, leading to the development of drug-resistant TB cases. In 2014, there were 480,000 new cases of multidrug-resistant (MDR) TB, comprising 3.3% of total new cases. While antimicrobial regimens for drug-susceptible TB require a minimum of 6 months treatment, MDR TB regimens last at least 21 months with an average success rate of only 50%[1]. Complicating matters further are the serious adverse side effects to antimicrobial therapy, which include liver and kidney toxicity as well as hearing and vision impairment[4]. Therefore, there is a need to explore alternate treatments such as the application of host-directed adjunct therapies to current antimicrobials to enhance drug efficacy as well as decrease the intensity and duration of treatment regimens.

II. Macrophage Infection by *Mycobacterium tuberculosis*

TB is an airborne disease transmitted by inhalation of aerosolized droplets containing Mtb from expectorating individuals with active disease[5]. Upon inhalation, Mtb is phagocytosed by resident alveolar macrophages where Mtb can undergo unrestricted replication[5-8]. Infected phagocytes migrate into lung interstitium and can disseminate to other organs via the lymphatic

system[5,7]. However phagocytes typically remain in the lungs and, in immune-competent individuals, form a granulomatous lesion composed primarily of mature macrophages followed by a combination of other leukocytes, lymphocytes, and epithelial cells[5,8]. While the granuloma serves as a method of Mtb sequestration and host protection, it is also considered a failed host immune response to bacterial clearance enabling Mtb survival[8].

Once encapsulated in a macrophage phagosome, Mtb secretes a number of lipid and protein effectors to prevent phagosomal maturation, the main microbicidal mechanism of macrophages[9]. Phagosomal maturation is the process where phagosomes interact with endosomes and lysosomes leading to the acidification of the Mtb-containing phagosome and exposure to proteolytic enzymes and reactive oxygen intermediates to clear the bacilli[10,11]. However, only 30% of Mtb-containing phagosomes are able to mature and destroy Mtb, providing a nutrient-rich host niche for Mtb persistence and replication (Figure 1.1)[8,10].

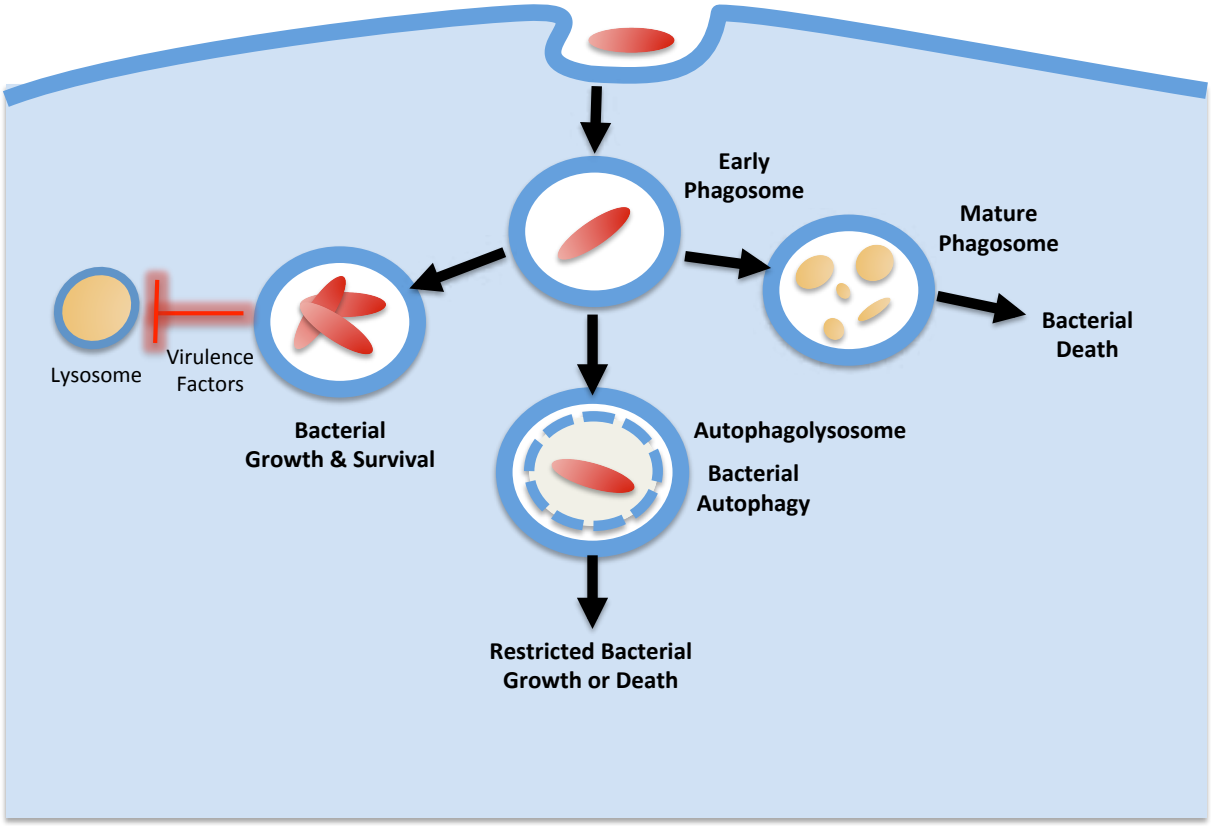

Figure 1.1 Intracellular fates of *M. tuberculosis*

III. Macrophage Polarization

A. Activation and Functionality

Macrophages alter their functionality through a process known as polarization. Depending on the signals they receive, macrophages are either classically activated and adopt a pro-inflammatory phenotype or alternatively activated, adopting an anti-inflammatory phenotype[12-14]. Classically activated, or M1, macrophages respond to type 1 inflammatory cytokines such as tumor necrosis factor alpha (TNFα) and microbial products enabling the production of nitric oxide (NO) and other reactive oxygen species (ROS) for antimicrobial activity[7,15]. Alternatively activated, or M2, macrophages respond to type 2 cytokines, such as interleukin 10 (IL-10), to resolve inflammation and promote tissue repair and angiogenesis[14,15]. While polarization results in two distinct cellular functional phenotypes, macrophages are highly plastic. Therefore, the same macrophage that drives a pro-inflammatory response may later aid in its resolution[13].

B. Mtb Infection

During acute Mtb infection, macrophages are classically activated by stimulation of toll-like receptors 2, 4, and 9[12,13,16]. However, Mtb can subvert this response both directly and indirectly via virulence factors, such as early secreted antigenic target protein-6 (ESAT-6)[12]. Additionally, Mtb can promote an M2 phenotype by increasing IL-10 production, rendering the cells poorly bactericidal with reduced antigen presentation capabilities[15]. Granulomas contain both macrophage polarities, however centrally located Mtb-infected macrophages are predominantly classically activated, while those uninfected along the periphery express the M2 phenotype[17,18]. This combination plays a dual role by (1) preserving lung tissue while sequestering the infection and (2) attempting to clear Mtb[7].

IV. Macrophage Metabolism

Macrophages are dependent on glucose as compared to fatty acids or amino acids to derive their energy[19]. However the way in which these cells metabolize glucose is dependent on

their state of polarity and activation. Therefore quiescent and M2 macrophages have a different metabolic profile than M1, activated macrophages (Figure 1.2).

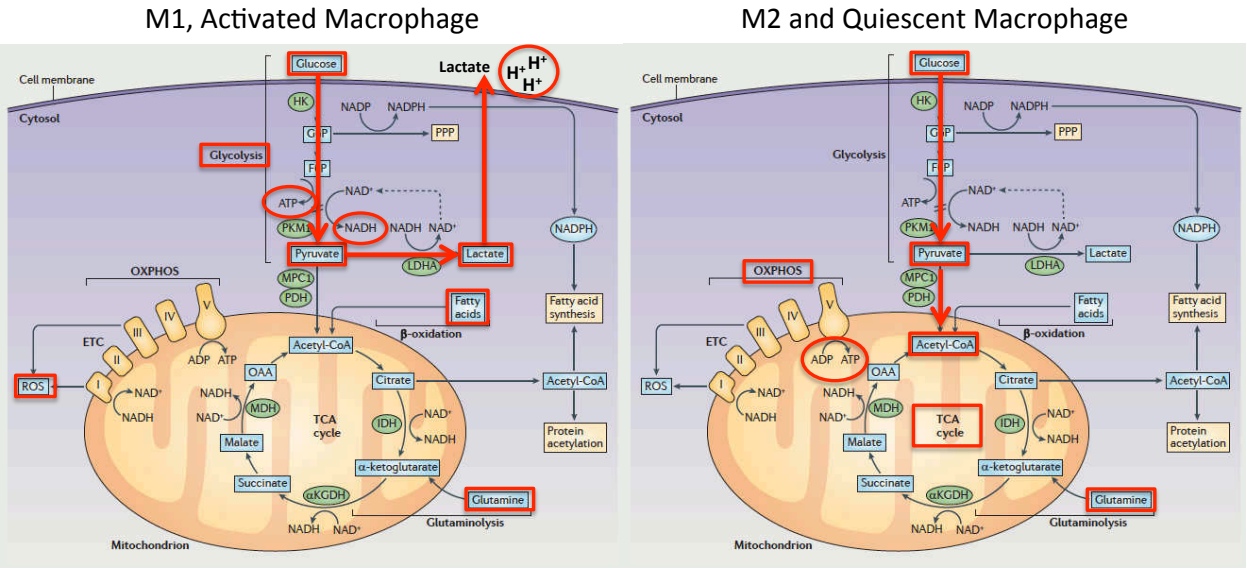

Figure 1.2 Macrophage metabolic pathways under different polarities. Image modified from Pearce, E. J. & Everts, B. Dendritic cell metabolism. *Nature reviews. Immunology* **15**, 18-29, doi:10.1038/nri3771 (2015)

A. Glucose Utilization Pathways

To generate adenosine triphosphate (ATP) from a single molecule of glucose, homeostatic cells utilize three pathways: (1) glycolysis, (2) the tricarboxylic acid (TCA) cycle, and (3) oxidative phosphorylation. Using a glucose transporter, glucose enters the cell cytoplasm and begins the oxidation process of glycolysis, where it is converted into two pyruvate molecules. This occurs via a 9-step process starting with the phosphorylation of glucose by the enzyme hexokinase. The net gain of this process is 2 ATP, 2 pyruvate molecules, and 2 reduced molecules of the coenzyme nicotinamide adenine dinucleotide (NADH). Pyruvate can convert to lactate by lactate dehydrogenase (LDH) within the cytoplasm or enter into the inner mitochondrial matrix and convert to acetyl coenzyme A (acetyl-CoA) by the pyruvate dehydrogenase complex. Within the mitochondria, acetyl-CoA can enter the TCA cycle, where it is further oxidized into 8 different substrate intermediates including citrate, α-ketoglutarate, succinate, and oxaloacetate. Under these conditions, the TCA cycle breaks down its intermediates to fuel energy production. During these transformations, four end products are

formed: 3 NADH coenzymes, 1 reduced flavin adenine dinucleotide ($FADH_2$) coenzyme, 2 CO_2 molecules, and 1 ATP per molecule of acetyl-CoA. Generated NADH is oxidized via complex I of the electron transport chain (ETC), also known as NADH dehydrogenase. Complex II, or succinate dehydrogenase, which is responsible for the reduction of $FADH_2$ in the TCA cycle, also contributes electrons to the ETC. The coenzyme oxidation releases electrons into the chain where they flow through coenzyme Q, complex III, cytochrome c, and complex IV, the final electron acceptor. This flow of electrons functions to form a proton gradient between the inner and inter-membrane mitochondrial spaces by driving hydrogen ions out of the inner mitochondrial matrix through ETC complexes I through IV. The polarization of this gradient drives ATP synthase to phosphorylate one molecule of adenosine diphosphate (ADP) into ATP. Overall, one molecule of glucose will generate approximately 36 ATP: 2 ATP from glycolysis, 2 ATP from the TCA cycle, and approximately 32 ATP from the ETC (Figure 1.2)[19].

Whereas quiescent and M2 macrophages primarily utilize oxidative phosphorylation, M1 activated macrophages will preferentially utilize glycolysis to generate ATP. While this metabolic shift was long known to occur under oxygen-poor conditions, it was noted in the 1920s by Otto Warburg that ATP generation from glycolysis could also occur in the presence of oxygen, terming this process “aerobic glycolysis”[16]. While glycolysis only produces 2 ATP, it is catabolically more efficient at generating energy as there are fewer processes required[20]. As pyruvate converts to lactate by lactate dehydrogenase, the NADH produced in glycolysis is reoxidized to NAD+, which can be reused in additional glycolytic processes to generate more ATP[19]. This shift allows the mitochondria to generate ROS through its ETC, and change the TCA cycle to an anabolic state where it can generate intermediates for fatty acid and amino acid biosynthesis that contribute to pro-inflammatory processes, such as the generation of prostaglandins via the arachidonic acid pathway[21,22]. Upon activation by Mtb, M1 macrophages will perform aerobic glycolysis to aid in their bactericidal function. Alternately, M2 macrophages

rely on oxidative phosphorylation to sustain their energy to serve their long-term regenerative function (Figure 1.2)[21].

B. Glucose Utilization in the Granuloma

Initially developed as a cancer diagnostic, positron emission tomography-computed tomography (PET-CT) has recently been investigated as a diagnostic for discerning active versus latent TB in patients (Figure 1.3 A)[23]. PET-CT defines areas of increased glucose demand using fluoro-18-deoxyglucose (^{18}FDG), a radioactive glucose analog[24]. While there are sites of normal physiologic glucose accumulation, such as the heart and brain, PET-CT also reveals pathologic sites of glucose accumulation where cells have increased metabolism due to inflammation or infection, such as the granuloma. Investigators determined that less ^{18}FDG uptake in the lesion is associated with latent disease while more ^{18}FDG accumulation is associated with active disease[18].

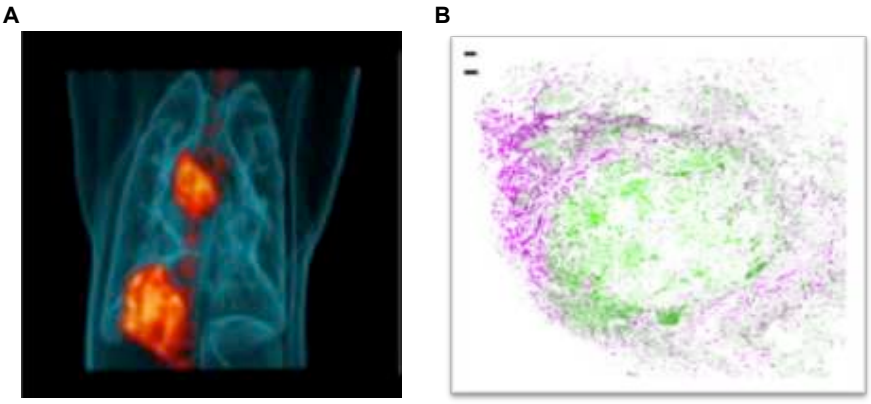

Figure 1.3 Glucose accumulation and macrophage polarization within non-human primate granulomas. (A) PET-CT scan showing ^{18}F-2DG accumulation and (B) immunohistochemistry of M1 (green) and M2 (purple) macrophages in granulomas. Images from Coleman, M. T. *et al.* PET/CT imaging reveals a therapeutic response to oxazolidinones in macaques and humans with tuberculosis. *Sci Transl Med* **6**, 265ra167, doi:10.1126/scitranslmed.3009500 (2014) and Marino, S. *et al.* Macrophage polarization drives granuloma outcome during Mycobacterium tuberculosis infection. *Infection and immunity* **83**, 324-338, doi:10.1128/IAI. 02494-14 (2015).

PET-CT has also been applied in atherosclerosis research to associate macrophage polarization within atherosclerotic plaques to ^{18}FDG accumulation. Increased accumulation was associated with M1 macrophages versus M2 macrophages[25]. Additionally, a recent study focused on computational modeling of a granuloma and polarity demonstrated that M1

macrophages composed the majority of infected cells within the lesion, while M2 macrophages reside around the periphery to protect surrounding tissues (Figure 1.3 B)[17]. Increased lactate levels have also been observed within the lungs of Mtb infected guinea pigs using high resolution magic-angle spinning nuclear magnetic resonance (HRMAS-NMR). This study determined that cells within the granuloma are primarily dependent on aerobic glycolysis for ATP generation[26]. Therefore it is likely that granulomatous macrophages within a patient with active disease are predominantly in an M1 polarized state and are primarily glycolytic compared to those within latent TB patients, which likely have a predominant M2 macrophage profile.

V. Chronic Hyperglycemia and Impaired Immune Function

Stress hyperglycemia and impaired glucose tolerance are associated with inflammation and infection, including active Mtb infection[27-30]. Approximately 13 to 45 percent of patients with active TB demonstrate impaired glucose tolerance, but only 2 to 7 percent are diagnosed with diabetes mellitus[31-33]. We have demonstrated that under both acute and chronic disease states Mtb infected guinea pigs have increased glucose levels in their blood sera that results in increased disease severity[34]. Chronic hyperglycemia during Mtb infection results in increased bacillary loads in patient sputum samples, increased lesion cavitation, and poorer treatment outcomes to anti-TB therapy[28].

On a cellular level, there remains conflicting evidence on the effects of high glucose conditions on macrophage function. While some studies demonstrate impaired pro-inflammatory responses to infection, others conclude an excessive inflammatory response to macrophage activation. Macrophages under hyperglycemic conditions have been described as having impaired microbicidal function including phagocytosis, cytokine secretion, and the production of ROS[35-38]. It is suggested that after long-term exposure to hyperglycemia M2 polarization may be the predominant macrophage phenotype[36,37]. However, there are other studies suggesting that increased extracellular glucose levels stimulate glycolysis, increasing M1 pro-inflammatory

responses[38,39]. Understanding these cellular responses may aid in our explanation of associated exacerbated disease severity to hyperglycemia.

VI. Mechanisms of Cell Death and Mtb Survival and Dissemination

There are three main classifications of cell death: necrosis, apoptosis, and autophagy. Necrosis is considered an inflammatory process due to its unregulated release of ROS and hydrolytic enzymes, and thus an undesirable cell death outcome[40]. Apoptosis and autophagy are regulated, self-contained processes that cause very little disturbance or inflammation to the surrounding environment, making them more favorable death mechanisms for granulomatous cells.

Necrosis

Necrosis is cell death via swelling (oncosis) and disruption of plasma membrane integrity followed by release of cytoplasmic contents[41]. Virulent Mtb strains, such as H37Rv, promote cellular necrosis as a means of bacillary dissemination[42]. Cells can also undergo necrosis after rapid ATP depletion, which leads to mitochondrial permeability transition via decreased activity of the ATP-sodium-potassium pump[43,44]. Inhibition of metabolic stress survival pathways, such as autophagy, can also lead to necrosis[44] .

Apoptosis

Apoptosis is cell death characterized by the morphologic features of cell shrinkage, membrane blebbing, and chromatin condensation (pyknosis)[41]. Mechanistically, apoptosis occurs via caspase protease activation either by the intrinsic mitochondrial pathway or the extrinsic death receptor pathway[41]. Two classes of caspases function within these pathways: (1) initiator caspases 2, 8 and 9, and (2) executioner caspases 3, 6 and 7[41]. While initiator caspases are activated according to extrinsic or intrinsic apoptotic pathways, executioner caspases are activated via proteolytic cleavage causing a conformational change into a mature protease[41]. Functions of executioner caspases include cleavage of complex I of the ETC to disrupt mitochondrial membrane potential and ATP production, the activation of DNAse to

cleave chromatin, and activation of actin cytoskeleton modulators responsible for the characteristic membrane blebbing[41].

The intrinsic pathway, the most common apoptotic pathway, is triggered by cellular stress such as DNA damage and insufficient ATP levels[41]. These stimuli induce mitochondrial outer membrane permeabilization (MOMP) by Bcl2 pro-apoptotic proteins Bax and Bak[41]. MOMP causes cytochrome c release into the cytoplasm where it can bind to apoptotic protease activating factor 1 (APAF1) to form the apoptosome and activate caspase 9, leading to executioner caspase activation and apoptosis (Figure 1.4)[41].

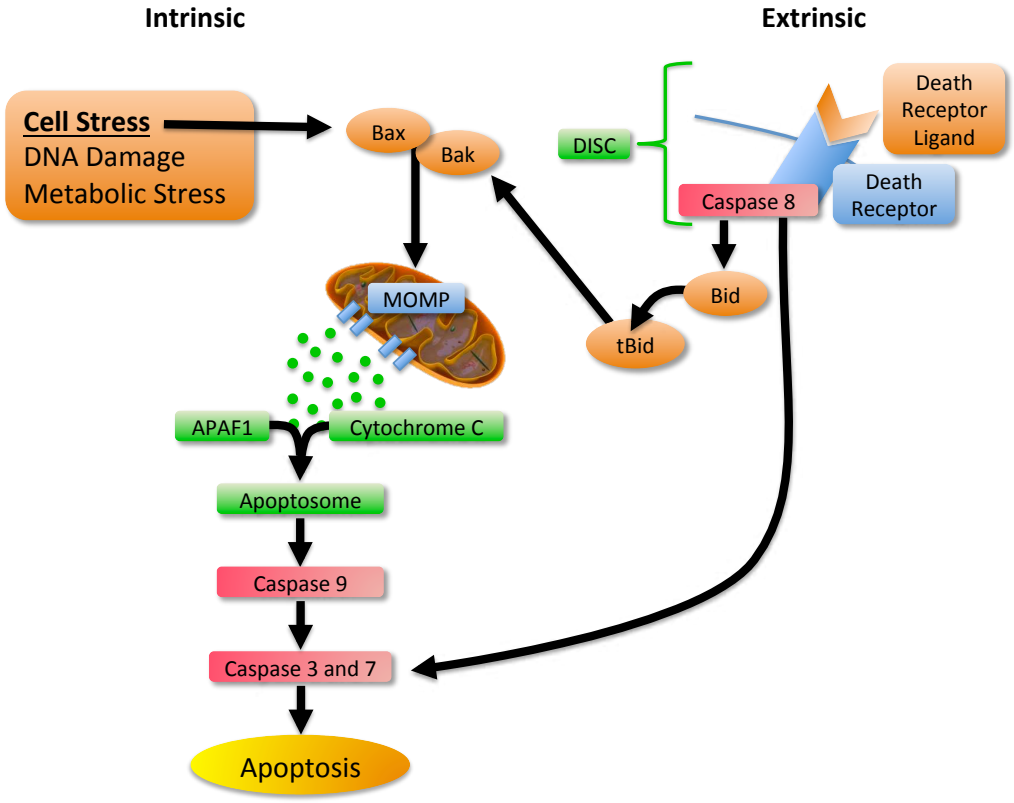

Figure 1.4 Intrinsic and extrinsic apoptotic pathways

The extrinsic pathway is signaled by the ligation of a death receptor, a subgroup of the tumor necrosis factor receptor family[41]. Once ligated, receptors such as Fas/CD95 or TNF-related apoptosis-inducing ligand receptor (TRAIL-R1/R2) form a caspase-activation platform, including caspase 8, known as a death inducing signaling complex (DISC)[41,45]. DISC can

directly activate executioner caspases 3 and 7 but more commonly will indirectly activate these caspases via cleavage of Bid, another pro-apoptotic protein, which subsequently activates Bax and Bak-mediated MOMP (Figure 1.4)[41].

Three benefits of undergoing apoptotic cell death are that (1) it eliminates Mtb's replicating host niche, (2) it can activate adaptive immunity through antigen presentation, and (2) it forces Mtb to reestablish itself within a naïve host cell, decreasing its chances of survival[42]. Therefore, apoptotic cell death, particularly via an intrinsic pathway, is considered a favorable mechanism of cell death under Mtb infection[40].

Autophagy

Autophagy, also known as "self-eating," is a process in which materials from within the cytoplasm are delivered to a lysosome for degradation and recycling. While this is a normal physiologic process to clear damaged organelles, it is also a cell stress survival mechanism such as under nutrient scarcity or intracellular bacterial infection (xenophagy)[41,46,47]. If autophagy is unsuccessful at ameliorating the stressor, autophagic machinery can promote cell death through a variety of mechanisms that have yet to be determined[41,46].

Autophagy begins by the formation of a double membrane structure known as the autophagosome via a three-step process (Figure 1.5 A). First is the activation of the pre-initiation complex Unc-51-like autophagy-activating kinase (ULK), which is negatively and positively regulated by the mammalian target of rapamycin complex I (mTORC1) and AMP-activated protein kinase (AMPK), respectively[41,42]. If activated by AMPK, the pre-initiation complex will recruit and activate the initiation complex, which is negatively regulated by the Bcl2 anti-apoptotic proteins Bcl2 and Bcl-xL[41]. Second is the elongation and closure of the autophagosome, which occurs in two ubiquitination-like reactions initiated by ATG7. The first reaction is conjugation of autophagy-related (ATG) proteins 5 and 12, which combine to form ATG16L1[42,46]. The second reaction is lipidation of ATG4-cleaved microtubule-associated protein light chain 3 (LC3-I) to phosphatidylethanolamine (PE) to form LC3-II. While the exact

mechanism has yet to be elucidated, these reactions continue until the phagophore membrane is fully expanded and enclosed. The final step is fusion of the autophagosome with a lysosome, forming an autolysosome, to recycle the vacuolar contents into usable resources, such as amino acids[41,42,46].

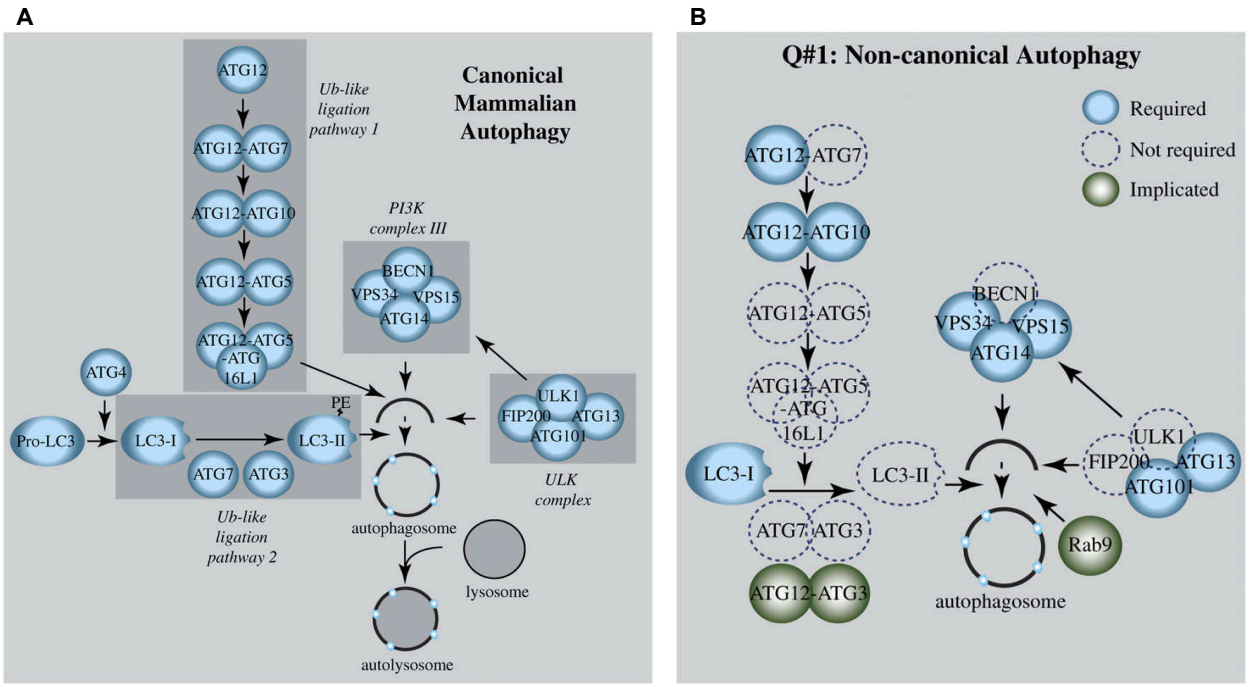

Figure 1.5 Classical and alternative autophagy pathways from Lindqvist, L. M., Simon, A. K. & Baehrecke, E. H. Current questions and possible controversies in autophagy. *Cell Death Discov* **1**, doi:10.1038/cddiscovery.2015.36 (2015).

In 2004, Gutierrez et al. was the first to suggest that autophagy-induction through either starvation or pharmacological means, such as rapamycin, could decrease Mtb survival within a macrophage by overriding Mtb inhibition of phagosome-lysosome fusion[47]. While this study laid the foundation for a promising target of host-directed therapy, autophagy has recently been questioned as the primary mechanism of intracellular bacillary control by cells of myeloid-lineage[48]. In 2015, Kimmey et al. determined that Mtb infected mice only had an increase in bacterial burden upon the deletion of ATG5, but not when other essential autophagy genes were deleted, such as ATG16L1[48,49]. However, there is much to be understood about autophagy and its mechanisms. A recent review by Lindqvist et al. describes these knowledge gaps

including the growing body of evidence suggesting a number of alternative mechanisms of autophagy (Figure 1.5 B). These mechanisms exclude what have classically been considered fundamental proteins, including those tested in the mouse models of Kimmey et al[46]. Therefore, as briefly suggested by its critics, autophagy may still play an important role in TB defense and clearance.

Mtb Survival and Dissemination

Mtb dissemination into neighboring cells occurs through host cell death via necrotic or apoptotic mechanisms, thus causing granuloma expansion (Figure 1.6)[11,42]. An increase in Mtb bacillary load is associated with necrotic cell death, allowing Mtb to spread and infect neighboring cells[7]. Also, increases in Mtb virulence are associated with extrinsic apoptotic cell death[40,50,51]. Under this condition, Mtb is able to survive within the blebbed apoptotic bodies that are subsequently engulfed by neighboring phagocytes, propagating the infection[52].

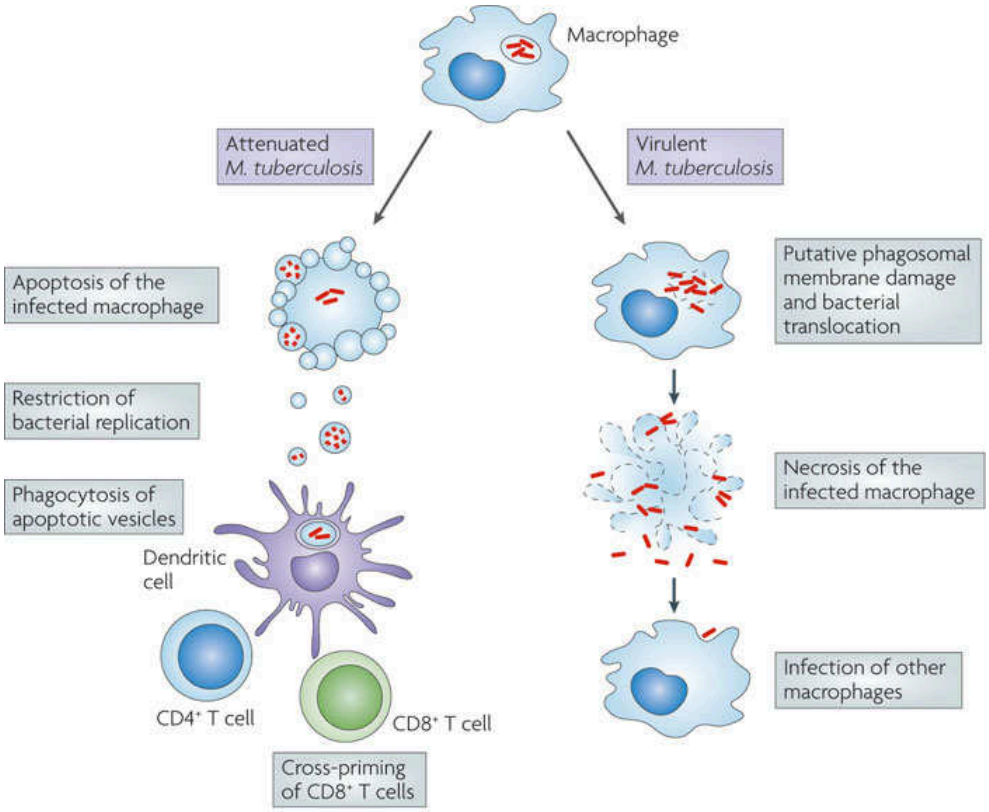

Figure 1.6 Mechanisms of cell death that promote bacterial dissemination from Behar, S. M., Divangahi, M. & Remold, H. G. Evasion of innate immunity by Mycobacterium tuberculosis: is death an exit strategy? *Nat Rev Microbiol* **8**, 668-674, doi:10.1038/nrmicro2387 (2010).

VII. Therapeutic Opportunities in Metabolic Regulation of Cell Death

Manipulation of glucose metabolism to induce host cell intrinsic apoptosis or autophagy-mediated cell death is a potential therapeutic intervention for inducing host-directed Mtb death and increasing antigen presentation.

Relationship of Glucose Metabolism to Apoptosis and Autophagy

Initiation of apoptosis and autophagy are metabolically signaled by the regulation of mTORC1 and AMPK, which are activated by alterations in ATP levels[43]. AMPK activation occurs upon ATP depletion, subsequently negatively regulating mTORC1, while promoting glycolysis[43]. Nutrient depletion along with AMPK signaling can initiate autophagy as a short-lived survival mechanism[43]. However, when autophagy is insufficient for survival and ATP levels are chronically low, the cell will become sensitized to both intrinsic and extrinsic apoptotic mechanisms[43,44]. Prolonged inhibition of mTORC1 causes degradation of Bcl2 anti-apoptotic proteins, priming the cell for mitochondrial apoptosis[43]. Additionally, glucose deprivation will sensitize the cell to death-receptor induced apoptosis, increasing caspase-8 dependent apoptosis[43].

Metformin

Metformin is the most frequently prescribed type II diabetic treatment worldwide due to its anti-hyperglycemic effects[53]. Systemically, the main target of metformin is the liver where it inhibits gluconeogenesis while stimulating glycolysis in hepatocytes, thus decreasing hepatic glucose output[53]. Metformin's effect is due to its partial inhibition of complex I of the ETC, causing a significant decrease in oxidative phosphorylation and subsequent ATP generation[53]. As described above, depletion of ATP leads to AMPK activation and potentially autophagy or apoptotic induction.

Recently, Singhal et al. have suggested metformin as an adjunct host-directed anti-TB therapy. It was shown to inhibit Mtb intracellular growth at concentrations of 1 mM and higher in human monocyte derived macrophages (hMDMs) as early as 24 hours post-infection. In these

experiments, it was confirmed that metformin upregulated AMPK and increased mitochondrial ROS for its cellular microbicidal functions. Scientists also demonstrated that hMDMs infected with *M. bovis* bacillus Calmette-Guérin (BCG), a commonly used avirulent Mtb surrogate, had increased autophagolysosome colocalization with BCG when treated with 2 mM metformin after 4 hours. However, prolonged exposure to metformin did not increase mitochondrial apoptotic cell death[54].

Use of metformin as a chemotherapeutic for cancer is also being explored. Many publications tout the antineoplastic effects associated with metformin treatment which include increased autophagy, apoptosis and cell cycle arrest, which demonstrate slowed rates of tumor growth and reduced tumor size (Figure 1.7 A)[55,56]. Most notable is the discovery that metformin increases its cytotoxic effects under a low glucose environment in a variety of cancer cell lines, while having little to no impact on non-cancerous cells[57-61]. The most common explanation for this paradigm is that metformin treatment increases glycolytic activity within already highly glycolytic cells[58,60,62]. Without excess extracellular glucose availability to maintain glycolytic ATP production in the cancerous cells, they may undergo autophagic or apoptotic cell death[58,60,62]. This suggests that the dual effect of metformin on the systemic and cellular level may function as a targeted therapy eliminating cells with an altered metabolic phenotype, while leaving physiologically healthy cells unaffected. This may also explain why metformin may be more effective in promoting cell death in a tumor environment where there are reduced concentrations of glucose compared to within the high glucose *in vitro* condition modeled by Singhal et al.

2-Deoxy-D-Glucose

2-Deoxy-D-glucose (2DG), is a glucose analog and competitive glycolytic inhibitor whose radiolabeled form, ^{18}FDG, is used in PET-CT as described above. As with glucose, when 2DG enters the cell, it undergoes phosphorylation by the first glycolytic enzyme, hexokinase. Unlike glucose, 2DG cannot be metabolized further once phosphorylated, thus inhibiting ATP production by glycolysis. Physiologically irrelevant levels of 2DG (above 1mM) do not activate

AMPK or cell death, demonstrating that cells can compensate for the loss of ATP production from glycolysis[63,64]. Additionally, a 5 mM 2DG treatment in Mtb-infected murine bone marrow derived macrophages revealed impaired cellular bactericidal function[65]. It is important to note that these studies were performed in hyperglycemic cell culture conditions and thus may not have made an impact in ATP glycolytic production. However, 2DG has also been shown to effectively activate AMPK by increasing cellular ROS and inducing autophagy to effectively clear intracellular bacteria (Figure 1.7 A)[45,66-70].

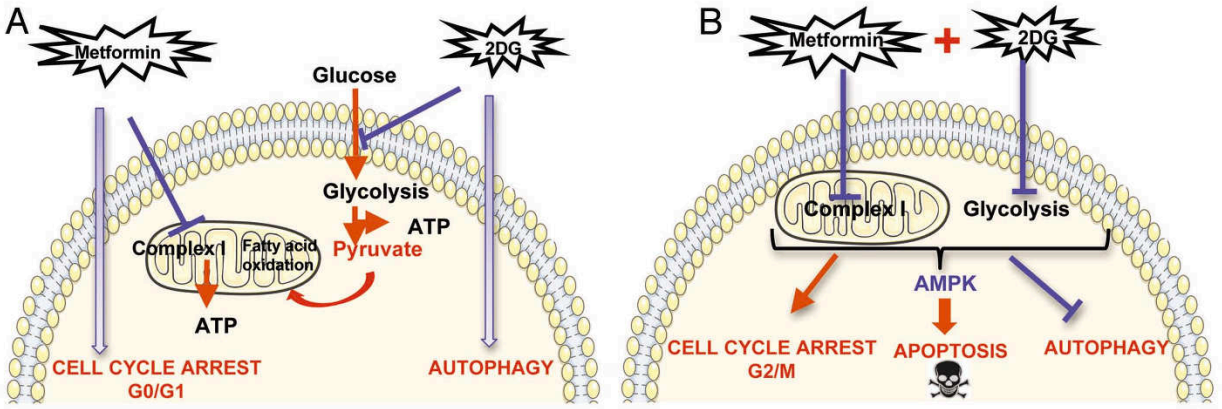

Figure 1.7 Metformin and 2DG mechanisms of action from Ben Sahra, I., Tanti, J. F. & Bost, F. The combination of metformin and 2-deoxyglucose inhibits autophagy and induces AMPK-dependent apoptosis in prostate cancer cells. *Autophagy* **6**, 670-671, doi: 10.1158/0008-5472.CAN-09-2782 (2010).

Potential Combination Therapy: Metformin and 2DG

Both metformin and 2DG have been suggested as enhancers of chemotherapeutic agents in cancer therapy. It has also been suggested that glucose deprivation via 2DG may increase the efficacy of metformin and thus require lower concentrations to achieve a therapeutic response. This recently introduced combination therapy resulted in significant cellular ATP depletion in prostate cancer cells and increased AMPK-mediated cell death, transitioning from autophagic to an intrinsic apoptotic pathway (Figure 1.7 B)[71]. The benefits of this combined therapy are that (1) no adverse side effects have been reported with either drug and (2) increased efficacy of metformin via glucose depletion has decreased cellular resistance

to chemotherapeutics rendering the drugs more effective at tumor elimination[71,72]. This therapy has slowly been gaining momentum, with several studies reporting favorable results[58,61,63]. However, this combined therapy has yet to be proposed in application to TB host-directed therapy. While one study demonstrated moderate increases in macrophage bactericidal functions using metformin (Singhal et al.) and another showed little influence with 2DG treatment alone (Gleeson et al.), it is possible that metformin and 2DG in combination may provide an enhanced synergistic effect. 2DG, as suggested by cancer treatment studies, may amplify the effect of metformin, which could increase anti-TB therapy efficacy leading to shorter and more effective TB treatment regimens.

VIII. The Guinea Pig Model for Tuberculosis

Since the late 19th century, guinea pigs have been the choice animal model for research in human bacterial infections, including TB[73]. Some of the similarities shared between humans and guinea pigs include pulmonary physiology, immunologic, hormonal and physiologic responses to infection, and the ability to generate a delayed-type hypersensitivity reaction after exposure to infection[73]. Additionally, guinea pigs are very susceptible to Mtb infection, which enables the development of a progressive infection upon implantation of a single tubercle bacillus, while displaying very similar lung pathology to that of humans[74,75]. The combination of the above factors makes the guinea pig an optimal animal model for the development and testing of new antimicrobial drugs and adjunct therapies[73]. Furthermore, our lab has demonstrated that Mtb-infected guinea pigs display non-diabetic hyperglycemia, making them ideal for testing the effect of metformin and 2DG on both cellular and systemic levels[34].

HYPOTHESIS AND SPECIFIC AIMS

Hypothesis

Mycobacterium tuberculosis-infected macrophages residing in a high glucose environment have increased glycolytic activity that can be targeted with metformin and 2-deoxyglucose to restore local glucose levels and induce apoptotic cell death to enhance bacterial clearance.

This hypothesis will be tested via the following aims:

Aim 1

Determine the effect of glucose concentration on macrophage glucose metabolism under activation and infection.

Aim 2

Determine the level of inhibition of metformin, 2-deoxy-glucose, and metformin-2-deoxy-glucose combined therapy on *M. tuberculosis* and macrophage oxidative phosphorylation and glycolysis.

Aim 3

Determine the effects of metformin, 2-deoxy-glucose, and metformin-2-deoxy-glucose combined therapy on *M. tuberculosis* viability and macrophage cell death.

MATERIALS AND METHODS

I. Guinea Pig Bone Marrow Derived Macrophages

Collection and Storage of Guinea Pig Bone Marrow Progenitor Cells

Strain 13 and Hartley guinea pigs (Charles River Breeding Laboratories, Inc., Wilmington, MA) were anesthetized by an intramuscular injection of 25mg/kg ketamine and 2mg/kg xylazine and euthanized using a sodium pentobarbital overdose by intraperitoneal injection. Following euthanasia, femurs and humerus were excised and cleared of all surrounding tissue using sterile gauze. Bones were soaked in 70% ethanol for one minute, followed by a 10 to 15 minute drying period. Sterile bone-cutting forceps removed both epiphyses on bones. Using a 22-gauge needle and 10 mL syringe filled with incomplete RPMI-1640, bone marrow progenitor cells were flushed out of diaphyses. Cells were collected in a 100x15mm petri dish and filtered through a 70 um cell strainer into a 50 mL conical tube. Conical tubes were centrifuged at 400 RCF for 5 minutes at room temperature. Supernatant was removed by aspiration and cells were resuspended in complete RPMI-1640, supplemented with 10% fetal bovine serum (FBS), 100 U/mL penicillin, and 100 ug/mL streptomycin. Cells were counted on a hemocytometer and viability was determined by via Trypan blue dye exclusion assay. Cells were resuspended at $1x10^7$ cells/mL in freezing media composed of 85% FBS and 15% dimethyl sulfoxide (DMSO) for cryopreservation. Cell suspension was immediately divided into 1 mL aliquots, placed in methanol-containing freezing chambers, incubated at -80°C overnight, and transferred to the gaseous liquid nitrogen phase for long-term storage.

Deriving Macrophages from Bone Marrow Progenitor Cells

Cryopreserved cells underwent a rapid thaw by gentle agitation in a preheated 37°C water bath for 2 minutes. Thawed cell suspension was immediately transferred to a 50 mL conical tube containing 30 to 40 mL of complete RPMI-1640 as described above. Cells were

centrifuged at 400 RCF for 5 minutes at room temperature. Supernatant was removed by aspiration and cells were resuspended in 20 mL of complete RPMI-1640 per thawed cryovial. A 10 mL of cell suspension was added to a 100x15mm non-tissue-culture-treated petri dish and supplemented with 20 ng/mL of human recombinant macrophage-colony stimulating factor (M-CSF; PeproTech, cat. no. 300-25). Cells differentiated over 7 days at 37°C in 5% CO_2. M-CSF was replenished 3 days after culture start.

Collecting and Plating Macrophages

On day 7, non-adherent cells and complete RPMI-1640 was removed by aspiration. Adherent cells were washed with 5 mL of pre-warmed calcium and magnesium-free Hanks Balanced Salt Solution (HBSS). Each petri dish received 3 mL CellStripper nonenzymatic cell dissociation solution (Corning, cat. no. 25-056-CI) and incubated for 15 min at 37°C in 5% CO_2. Remaining adherent cells were detached by scraping. Final cell suspensions were pooled in a 50 mL conical tube. Petri dishes were washed twice with HBSS and washes were added to pooled cells. Cell suspensions were centrifuged at 400 RCF for 5 minutes at room temperature. Supernatant was removed by aspiration and cell pellet was resuspended in 3 to 5 mL complete RPMI-1640 media containing M-CSF. Cells were counted on a hemocytometer and viability was determined by Trypan blue dye exclusion assay. Cells were either plated in a 48-well sterile, non-tissue-culture treated plate at 300,000 cells per well or at 65,000 cells per well in Seahorse XFp Cell Culture miniplates (cat. no. 103025-100) pre-coated with poly-L-lysine (Sigma, cat. no. P4707).

Culture Conditions

As we have previously published, guinea pigs display increased serum glucose levels 60 days post-Mtb infection compared to their pre-infected state. More specifically, serum glucose levels increase from 100 mg/dL (5mM) to 200 mg/dL (11mM). To model the two glucose conditions, cells were cultured in a glucose-free DMEM (ThermoFisher, cat. no. A1443001) containing M-CSF and supplemented with 10% dialyzed FBS, 2mM glutamine, and either 5mM

or 11mM cell-culture grade glucose solution (Sigma, cat. no. G8769) to mimic euglycemic and hyperglycemic conditions, respectively, as observed in our guinea pig model. After preparation, all media was sterile-filtered by a 0.22um filter. Cell treatments included 1,1-dimethylbiguanide hydrochloride (Metformin; Sigma, cat. no. D150959) and/or 2-deoxy-D-glucose (2DG; Sigma, cat. no. D6134).

II. Macrophage Infection Model

Non-infectious Activation Model

A 10mg/mL suspension of zymosan A from *Saccharomyces cerevisiae* (Sigma, cat. no. Z4250) was prepared in sterile 1x phosphate buffered solution (PBS). Macrophages were activated by incubation with 100 ug/mL of zymosan for 4 hours at 37°C in 5% CO_2.

Mtb Infection Model

Macrophages were incubated with *Mycobacterium tuberculosis* strain H37Rv (Mtb) at a multiplicity of infection (MOI) of 5:1 for 4 hours at 37°C in 5% CO_2. Cells were washed three times with pre-warmed 1x PBS followed by a 1-hour incubation in complete DMEM supplemented with 100ug/mL gentamycin. Cells were washed once with pre-warmed 1x PBS and placed in final experimental media conditions.

III. Metabolic Analysis

We utilized two different technologies to assess cellular metabolism. The first was a high resolution respirometer, also known as the Oxygraph 2k (Oroboros Instruments). While this instrument has high sensitivity and precision, it is low throughput and cannot undergo the Biosafety Hazard Level 3 (BSL3) decontamination procedure. Therefore, this instrument was utilized for initial model development and the non-infectious activation model outside of the BSL3 facilities. The second technology was the 8-well extracellular flux analyzer, the Seahorse XFp (Seahorse Biosciences). Due to the BSL3 compatibility and high throughput capabilities, this instrument performed metabolic analysis on Mtb-infected cells.

From both instruments, we obtained two simultaneous measurements: (1) the cellular oxygen consumption rate and (2) the extracellular acidification rate. The oxygen consumption rate, or OCR, is an indirect measure of oxidative phosphorylation as this is the primary cellular process requiring oxygen. The extracellular acidification rate, or ECAR, is an indirect measure of glycolysis. The glycolytic byproducts, lactate and hydrogen ions, are secreted by the cell which cause a decrease in culture media pH. While the Oxygraph 2k directly measures these two parameters using an oxygen sensor and pH probe, the Seahorse XFp utilizes fluorophores to measure the excitation and emission spectra produced by changes in dissolved oxygen and proton concentrations.

To test the metabolic parameters of a cell sample, we added a series of substrates that systematically shut down or promoted different components of mitochondrial respiration or glycolysis. When the cell samples are first inserted into the Oxygraph 2k or the Seahorse XFp, they are suspended in a non-buffered Dulbecco's Modified Eagle's Medium Base, supplemented with 10mM glucose, 2mM pyruvate, and 2mM L-glutamine, 7.4 pH. Here, OCR and ECAR measurements provide the cellular metabolic baseline. Next, 0.5 uM of rotenone and antimycin A, inhibitors of complexes I and III of the electron transport chain, are added to stop mitochondrial respiration which causes a decrease in OCR. Here, ECAR either remains stable if cells are primarily glycolytic or will increase, demarcating a shift in metabolism from oxidative phosphorylation to glycolysis for ATP generation. The second substrate added is 50mM 2DG, a competitive inhibitor of glucose metabolism. With 2DG entering the cell at five times the rate of glucose, ATP production via glycolysis stops, thus decreasing cellular ECAR. Both substrate injections enable the calculation of cellular respiration and glycolysis.

IV. Fluorescent and Colorimetric Assays

Lactate Production Assay

We used the Picoprobe L-Lactate Assay Kit by Abcam (cat. no. ab169557) as a secondary measure of cellular glycolytic activity. Here, L-Lactate, the main stereoisomer

produced by lactate dehydrogenase, is oxidized to form an intermediate that reacts with a probe to fluoresce. To begin, Lactate Enzyme and Substrate Mixes were reconstituted per kit instructions followed by the dilution of the 10mM Lactate Standard to 25uM to produce a standard curve. Lactate standards and 1:400 diluted cell sample supernatants were added to a black, clear-bottom 96-well microplate in duplicate. Next, reaction and background control mixes were added. Using the Gen5™ Reader Control and Data Analysis Software, the microplate was programmed [60]incubate at room temperature for 30 minutes within the Synergy 2 Multi-Mode Reader by BioTek, followed by fluorescent measurement using the 530/25 nm and 590/35 nm excitation and emission filters respectively. After all values were obtained, the 0 pmol lactate standard value was subtracted from all other standard and sample values. If the background control was significantly, it was also subtracted from the sample readings. A lactate standard curve was generated in GraphPad Prism and sample concentration values were calculated per kit instructions.

Minimum Inhibitory Concentrations of 2DG and Metformin Treatment on Mtb Growth

A frozen aliquot of H37Rv Mtb was brought to room temperature and resuspended in 10 mL of 7H9 broth, supplemented with 0.05% Tween 80 and 10% OADC. Mtb incubated for 48 hours at 37°C and suspension turbidity was matched to 1/25 of a McFarland no. 1 turbidity standard (OD 0.0156nm). Dilutions (1:2) of 2DG and Metformin were performed in a sterile 96-well plate in 7H9 media, or complete DMEM containing 5mM or 11mM glucose concentrations. Final well concentrations of 2DG ranged from 8.75 mM to 0 mM, while metformin concentrations ranged from 3 mM to 0 mM. Diluted Mtb (100 uL) was added to all wells. Plate was sealed with parafilm and incubated for 5 days at 37°C. On day 5, 50 uL of a 1:1 dilution of alamar blue and 10% Tween 80 was added to all wells and plate was resealed. After an additional 24 hour incubation at 37°C, the plates were read in the Synergy 2 Multi-Mode Reader at OD 570nm and 600nm to determine levels of bacterial growth.

V. Survival Assays

Trypan Blue Exclusion Assay

Complete media was removed from macrophage cultures and saved in a 15 mL conical tube. Next, macrophages were rinsed with 500 uL of 1x PBS and washes were combined with media in conical tube. CellStripper nonenzymatic cell dissociation solution was added to wells (250 uL) and incubated for 15 minutes at 37°C in 5% CO_2. Macrophages were detached by gentle scraping with a 1 mL syringe plunger. Cell suspension was combined with media and washes in conical tube. Wells were washed twice with 1 mL complete DMEM and added to conical tube. Tubes were centrifuged at 400RCF for 5 minutes at room temperature. Supernatant was decanted and cell pellets were resuspended in 500 uL complete DMEM. Cell suspension (10 uL) was combined with 10 uL of 0.4% Trypan Blue Solution. The combined solution was inserted onto a hemocytometer (10 uL) and cells including and excluding Trypan blue were quantified under the microscope.

Autophagy/Apoptosis/Necrosis Assay

The following reagents were used in this assay: monodansylcadaverine (MDC; Sigma, cat. no. 30432), FAM FLICA™ Caspase 3 & 7 reagent (Immunochemistry, cat. No. 94), SYTOX® AADvanced™ Dead Cell Stain (ThermoFisher, cat. no. C10427), and APC Annexin V (Biolegend, cat. no. 640920). To begin, 0.05mM MDC and caspase 3 and 7 reagent were added to cell cultures followed by a 1 hour incubation at 37°C in 5% CO_2. Next, cell cultures were detached from 48-well plates using CellStripper as described above, washed twice in 1x apoptosis wash buffer, and resuspended in 200 uL 1x annexin binding buffer containing 1:20 APC Annexin V. Tubes incubated for 15 minutes at room temperature. 1 uM of SYTOX® AADvanced™ Dead Cell Stain was added for the last 5 minutes of the APC Annexin V staining duration. Samples were immediately placed on ice prior to analysis. Cells treated with 8 uM rapamycin, 20 uM camptothecin, and 0.005% Triton x 100 for 12 hours served as positive

controls for autophagy, apoptosis, and necrosis respectively. Flow cytometric analysis was performed on the BD™ LSR II using BD FACSDiva™ software.

Mtb Survival Assay

Macrophages were detached from the 48-well plate using CellStripper nonenzymatic cell dissociation solution as described above and counted using Trypan blue dye exclusion assay. Once quantified, cells were lysed in 0.1% Triton X 100 at 37°C for 10 minutes. 1:10 serial dilutions were made in sterile 1x PBS and plated on 7H11 agar plates, supplemented with OADC, Carbenicillin, and Cyclohexamide. Plates incubated at 37°C and colony-forming units were quantified after 21 days.

VI. Statistical Analysis

GraphPad Prism 7 and SAS 9.4 software were used for statistical analysis with an alpha equal to 0.05. A two-way factor analysis of variance (ANOVA) was performed on all data sets to determine differences between cellular infection and treatment-status and differences within these groups over time. A Tukey's range test was used to determine statistical differences among treatment groups at a specific time point and within each treatment group over time. Dunnett's test was employed for dose response curves and Trypan blue dye exclusion assays for comparison of treatment groups to an untreated control. Use of a three-way factor ANOVA determined statistical significance between 100mg/dL and 200mg/dL glucose conditions on different treatments.

RESULTS

Aim 1: *Determine the effect of glucose concentration on macrophage glucose metabolism under activation and infection.*

Using the non-infectious activation and Mtb infection models, basal respiration and glycolysis were assessed 4 hours after stimulation using the Oxygraph 2k and Seahorse XFp analysis (**Figure 2.1**). Zymosan A stimulated GPBMDMs increased basal respiration under a 100mg/dL glucose condition (P<0.0002), while slightly elevating basal respiration in a 200mg/dL glucose condition (**Fig 2.1 A**). Glycolytic activity increased under both glucose conditions after 4 hours of zymosan A stimulation (P<0.0001) (**Fig 2.1 C**).

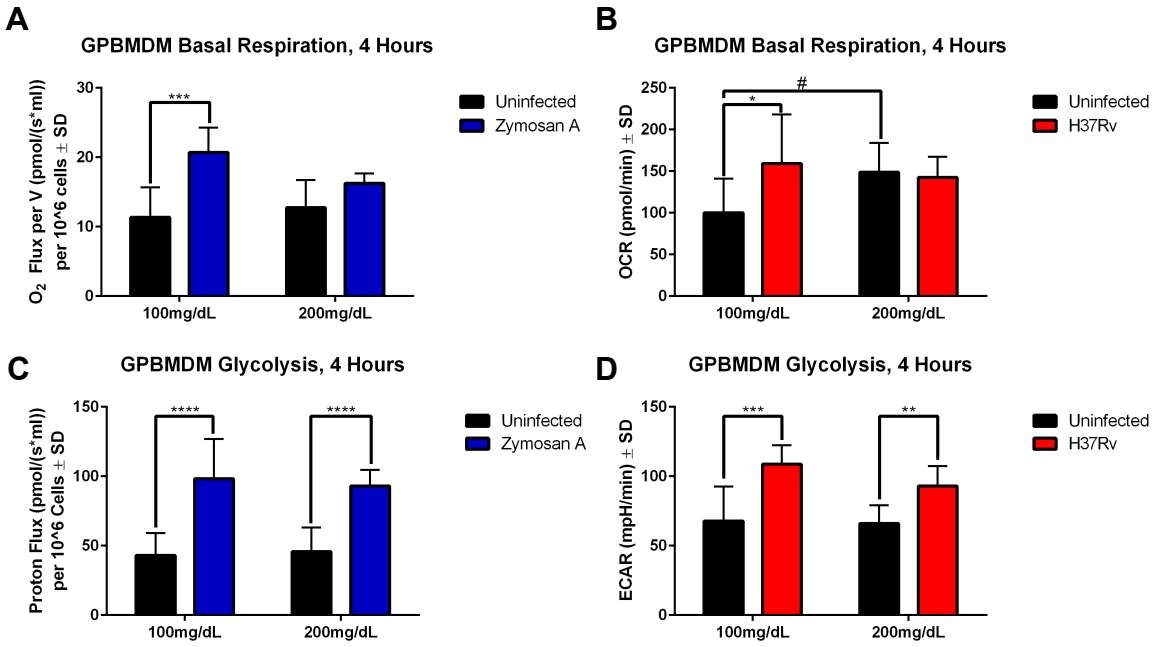

Figure 2.1 Macrophage activation and infection increases basal oxygen consumption and glycolytic rate. GPBMDM basal respiration under (A) zymosan A stimulation or (B) Mtb infection. GPBMDM glycolysis under (C) zymosan A stimulation or (B) Mtb infection. Data is expressed as (A) O_2 flux per volume in pmol/(s*mL) per 10^6 cells ± standard deviation (SD), (B) oxygen consumption rate (OCR) in pmol/min per 65,000 cells ± SD, (C) proton flux in pmol/(s*mL) per 10^6 cells ± SD, and (D) extracellular acidification rate (ECAR) in mpH/min per 65,000 cells ± SD. (A and C) n=7 in uninfected cells and n=5 in zymosan A stimulated cells, (B and D) n=6 in uninfected cells and n=6 in Mtb infected cells. * and # =P≤ 0.05, ** =P≤ 0.01, ***=P≤ 0.001, ****=P≤ 0.0001.

Mtb-infected GPBMDMs displayed a similar metabolic profile to zymosan A stimulated GPBMDMs (**Fig 2.1 B and D**). Under a 100mg/dL glucose condition, Mtb-infection increased GPBMDM basal respiration ($P<0.0113$) (**Fig 2.1 B**). In uninfected GPBMDMs, exposure to a 200mg/dL glucose environment from a 100mg/dL glucose environment increases basal respiration ($P<0.0254$) (**Fig 2.1 B**). Mtb-infected GPBMDMs increase their glycolytic activity compared to uninfected GPBMDMs ($P<0.0001$, $P<0.0052$) (**Fig 2.1 D**). These data demonstrate that macrophage activation and infection increase basal respiration and glycolytic rates compared to uninfected macrophages, and that a high glucose environment impairs the respiratory response to activation or infection.

Uninfected and Mtb-infected GPBMDMs basal respiration and glycolytic activity were analyzed over 72 hours using the Seahorse XFp and lactate production assay. In 100mg/dL glucose conditions, infected GPBMDMs had increased basal respiration compared to uninfected GPBMDMs beginning 4 hours post-infection ($P<0.0113$) and lasting for at least 72 hours (**Fig 2.2 A**). Under 200mg/dL glucose conditions, infected GPBMDM basal respiration remained similar to uninfected GPBMDMs, except at 48 hours post-infection where it peaked similarly to 4 hours post-infection ($P<0.0122$) (**Fig 2.2 B**). Significant decreases in basal respiration were noted in both uninfected and infected GPBMDMs under a 200mg/dL glucose condition over time ($P<0.0001$) (**Fig 2.2 B**). Under both 100 and 200mg/dL glucose conditions, glycolytic activity peaked 48 hours post-infection (200mg/dL =$P<0.0004$) and declined by 72 hours (100mg/dL =$P<0.003$, 200mg/dL =$P<0.0001$) (**Fig 2.2 C and D**). However, glycolytic activity in infected cells under a 100mg/dL glucose condition remained elevated after 48 hours, while those under a 200mg/dL glucose condition did not (**Fig 2.2 C and D**).

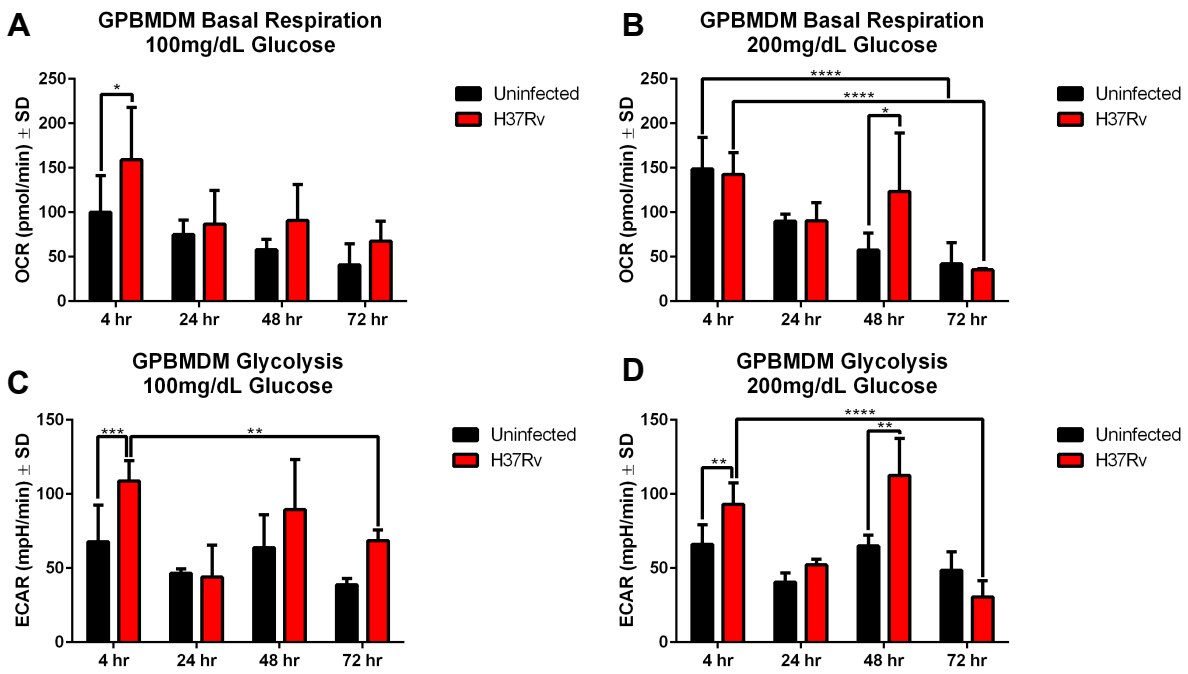

Figure 2.2 Mtb-infected macrophages have different metabolic profiles under normal and high glucose conditions. GPBMDM basal respiration in (A) 100mg/dL and (B) 200mg/dL glucose conditions. GPBMDM glycolysis in (C) 100mg/dL and (D) 200mg/dL glucose conditions. Data is expressed as (A and B) OCR in pmol/min per 65,000 cells ± SD, (C and D) ECAR in mpH/min per 65,000 cells ± SD. (A and C) n=6, 2, 3, and 3 in uninfected cells and n=8, 4, 3, and 3 in infected cells, (B and D) n=6, 2, 3, and 2 in uninfected cells and n=6, 3, 3, and 3 in infected cells at specified time points. *=P≤ 0.05, ** =P≤ 0.01, ***=P≤ 0.001, ****=P≤ 0.0001.

A lactate production assay was used to validate cellular glycolytic activity. Overall, infected GPBMDMs produced more lactate than uninfected GPBMDMs (**Fig 2.3**). Lactate accumulated more rapidly in infected GPBMDMs under a 100mg/dL glucose condition than those in a 200mg/dL glucose condition. This was most notable 48 hours post-infection where infected GPBMDMs under a 100mg/dL glucose condition had significantly greater lactate accumulation than those under a 200mg/dL glucose condition (P<0.0319) (**Fig 2.3**). Compared to uninfected GPBMDMs, infected GPBMDMs had significantly more lactate accumulation 48 and 72 hours post-infection under a 100mg/dL glucose condition (P<0.0003 and P<0.0081) (**Fig 2.3 A**). In a 200mg/dL glucose condition, lactate accumulation in infected GPBMDMs was also significantly greater than in uninfected GPBMDMs 72 hours post-infection (P<0.0009) (**Fig 2.3**

B). These data suggest that GPBMDM glycolytic responses to infection are also impaired under a high glucose environment.

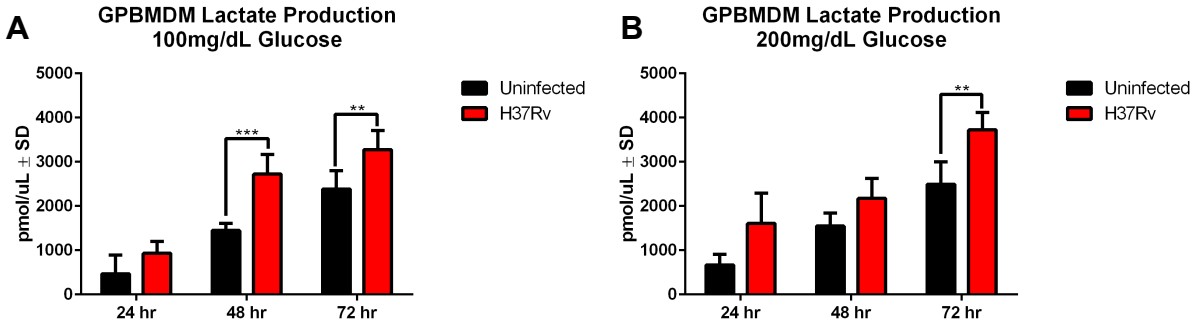

Figure 2.3 Mtb-infected macrophages have different levels of lactate accumulation. GPBMDM lactate production in (A) 100mg/dL and (B) 200mg/dL glucose conditions. Data is expressed as pmol/uL lactate ± SD. n= 3, 3, and 4 in uninfected cells and n=3, 3, and 3 in infected cells at specified time points. ** =P≤ 0.01, ***=P≤ 0.001.

Aim 2: *Determine the level of inhibition of metformin, 2-deoxy-glucose, and metformin-2-deoxy-glucose combined therapy on M. tuberculosis and macrophage oxidative phosphorylation and glycolysis.*

After infecting GPBMDMs, metformin and/or 2DG were added to cell cultures. According to pharmacokinetic/pharmacodynamic studies, metformin in blood sera reaches a peak concentration of 12uM, while 2DG concentration peaks at 700uM[76,77]. Concentrations above and below these blood sera levels were chosen for formation of dose response curves in infected GPBMDMs. Dose response curves demonstrated that metformin treatment alone decreases basal respiration and increases glycolysis in a dose-dependent manner after 24 hours (**Fig 2.4 A and B**). 1.2mM metformin was the only dose to have statistically significant inhibition of basal respiration after 4 hours of treatment (P<0.0295) (**Fig 2.4 A**). 2DG treatment decreased basal respiration and glycolysis dose-dependently after 4 and 24 hours (**Fig 2.4 C and D**). While there were no statistically significantly decreases in basal respiration, glycolysis decreased with 2DG treatment after 4 hours starting at 700uM (P<0.0001) (**Fig 2.4 D**). 3.5mM, 7mM, and 35mM concentrations of 2DG also demonstrated statistically significant decreases in glycolysis after 4 hours of treatment (P<0.0277, P<0.0456, and P<0.0148) (**Fig 2.4 D**).

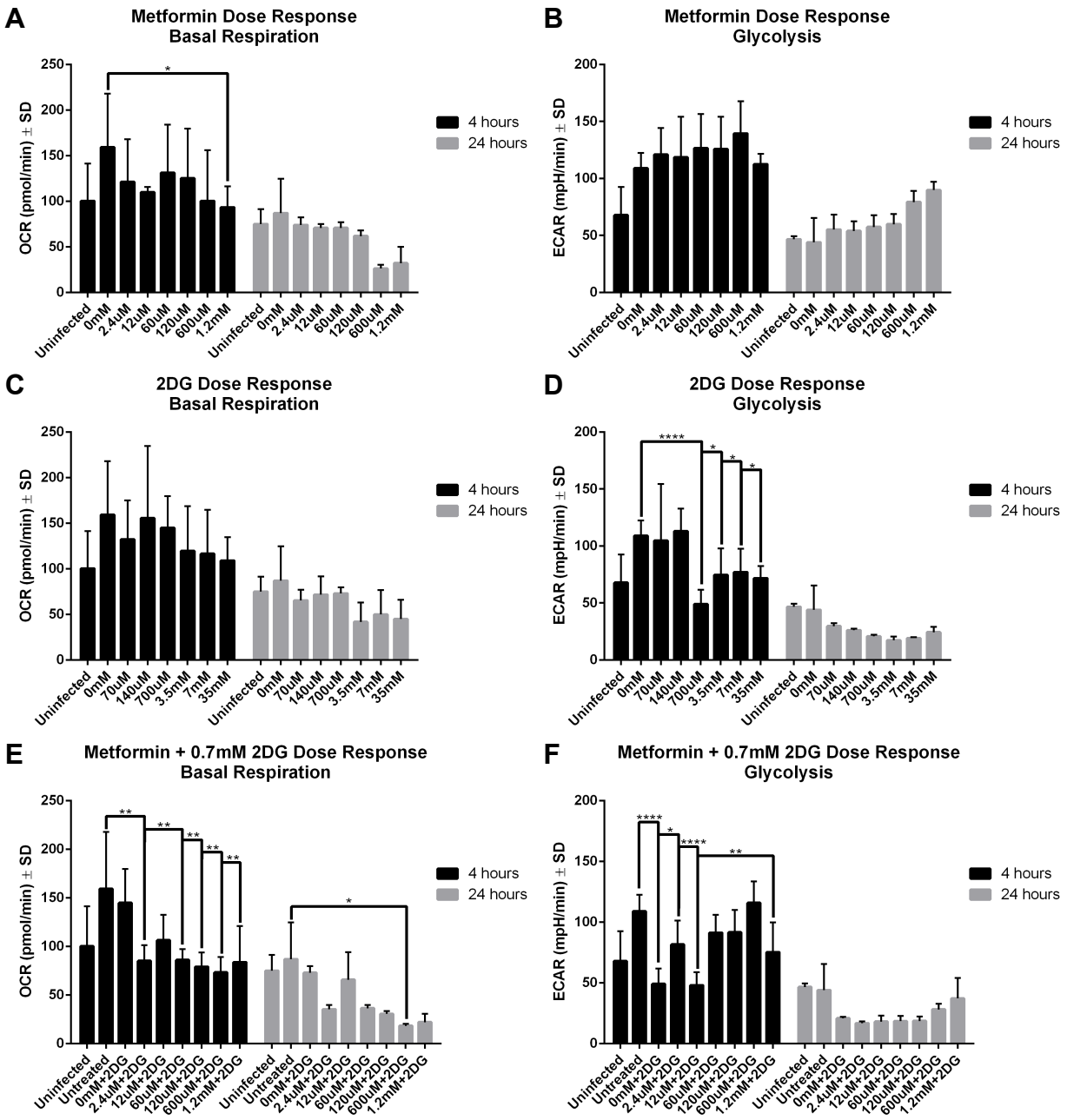

Figure 2.4 Metformin, 2DG, and Metformin-2DG dose response curves 4 and 24 hours post-infection and treatment in a 100mg/dL glucose condition. (A) Basal respiration and (B) glycolysis in uninfected (n=6) and infected GPBMDMs after metformin treatment at doses 0mM (n=8), 2.4uM (n=3), 12uM (n=4), 60uM (n=3), 120uM (n=3), 600uM (n=3), and 1.2mM (n=4). (C) Basal respiration and (D) glycolysis in uninfected (n=6) and infected GPBMDMs after 2DG treatment at doses 0mM (n=8), 70uM (n=3), 140uM (n=3), 700uM (n=5), 3.5mM (n=3), 7mM (n=3), and 35mM (n=3). (E) Basal respiration and (F) glycolysis in uninfected (n=6) and infected GPBMDMs (n=8) after treatment with 700uM 2DG and metformin doses 0mM (n=5), 2.4uM (n=3), 60uM (n=3), 120uM (n=3), 600uM (n=3), and 1.2mM (n=3). Data is expressed in (A, C, and E) OCR in pmol/min per 65,000 cells ± SD and (B, D, and F) ECAR in mpH/min per 65,000 cells ± SD. *=P≤ 0.05, ** =P≤ 0.01, ***=P≤ 0.001, ****=P≤ 0.0001.

Using the physiologically relevant 700uM 2DG dose, concentrations of metformin tested singly were also tested in combination to determine the optimal dual treatment for inhibition of both basal respiration and glycolysis (**Fig 2.4 E and F**). Overall, combined metformin and 2DG treatment decreased cellular basal respiration after 24 hours more effectively than singly treated GPBMDMs (**Fig 2.4 E**). After 4 hours, 2.4uM, 60uM, 120uM, 600uM, and 1.2mM metformin doses in combination with 2DG significantly inhibited basal respiration ($P<0.0069$, $P<0.0079$, $P<0.0031$, $P<0.0014$, and $P<0.0058$) (**Fig 2.4 E**). After 24 hours, 600uM metformin in combination with 700uM 2DG was most effective at inhibiting basal respiration ($P>0.0357$) (**Fig 2.4 E**). 2.4uM, 12uM, and 1.2mM metformin doses in combination with 2DG also significantly inhibited glycolysis after 4 hours ($P<0.0316$, $P<0.0001$, and $P<0.005$) (**Fig 2.4 F**). However, after 24 hours 2DG inhibited glycolysis regardless of metformin concentration (**Fig 2.4 F**). Collectively, the combination of 600uM metformin and 700uM 2DG was most effective at inhibiting both basal respiration and glycolysis in infected GPBMDM. While this dose of metformin is greater than the physiologic blood sera maximum concentration, it is less than half the concentration typically used in metformin *in vitro* studies and well below the concentration needed to cause metformin-associated lactic acidosis[54,60,71].

Three metformin and 2DG MICs were performed using serial dilutions of each compound. Maximal metformin and 2DG concentrations were 3mM and 8.75mM, respectively. Mtb growth was not inhibited by either compound, but was inhibited by its growth media. 7H9 broth promoted bacterial growth, while DMEM inhibited bacterial growth regardless of metformin and/or 2DG being present (**Fig 2.5 A**). Metabolic analysis on $2.5x10^6$ CFU of Mtb within DMEM media (over 7 times the amount used to infect GPBMDMs) revealed very little basal respiration and glycolytic activity (**Fig 2.5 B**). These results indicate that Mtb growth is unaffected by metformin and/or 2DG treatment and that extracellular Mtb metabolic activity did not confound the GPBMDM metabolic analysis.

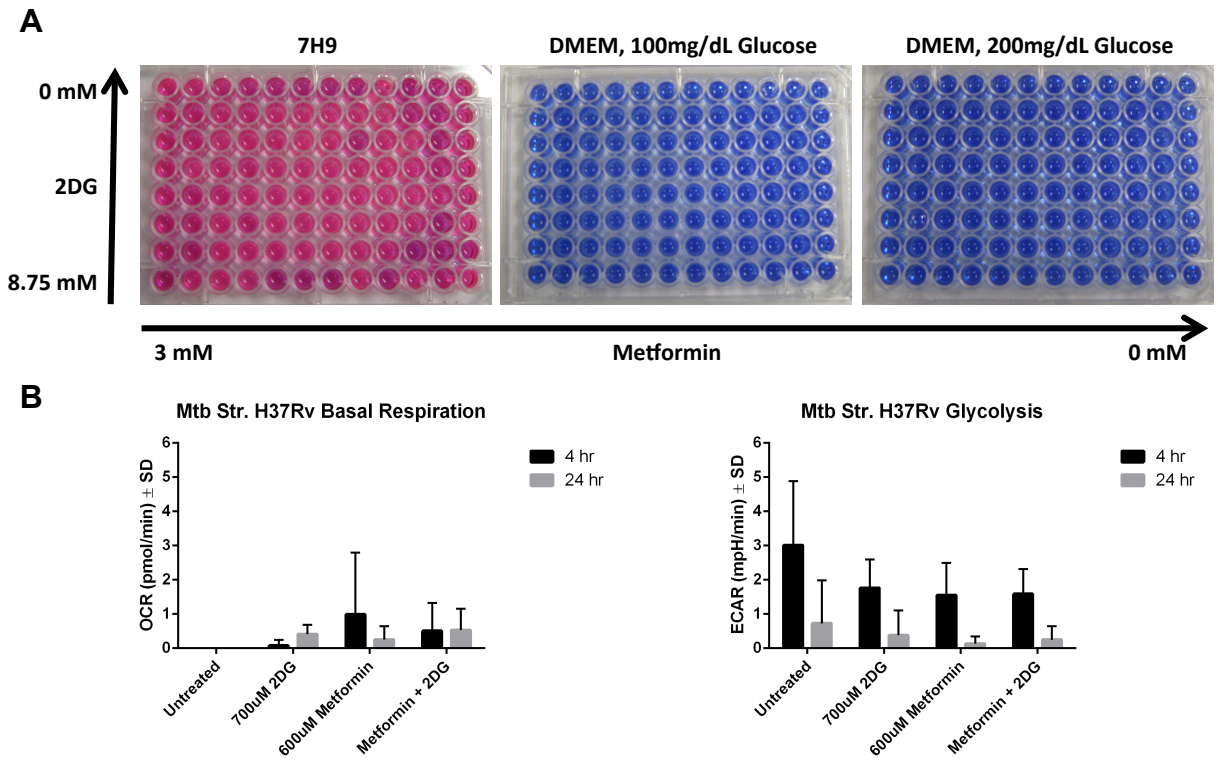

Figure 2.5 Mtb growth and metabolism are not affected by metformin, 2DG, or metformin-2DG combined treatments. (A) Mtb growth in 7H9 broth or DMEM media containing 100 or 200mg/dL glucose, treated with metformin and/or 2DG. (B) Basal respiration and glycolysis of $2.5x10^6$ CFU Mtb after 4 and 24 hours of metformin and/or 2DG treatment (n=3).

Uninfected and infected GPBMDMs were treated with 600uM metformin and 700uM 2DG under 100 and 200mg/dL glucose conditions. Significant inhibition of basal respiration in uninfected GPBMDMs occurred 4 hours after metformin-2DG treatment in both glucose conditions ($P<0.0333$, $P<0.0001$), and also occurred 24 hours after treatment in the 200mg/dL glucose condition ($P<0.0068$) (**Fig 2.6 A and B**). In uninfected GPBMDMs, metformin-2DG treatment became ineffective at inhibiting basal respiration after 24 hours (**Fig 2.6 A and B**). Under a 100mg/dL glucose condition, metformin-2DG treatment of infected GPBMDMs suppressed basal respiration as early as 4 hours after treatment and was sustained for 72 hours ($P<0.0025$, $P<0.0484$) (**Fig 2.6 C**). Under a 200mg/dL glucose condition, metformin-2DG treatment did not effectively suppress basal respiration until 48 hours after treatment ($P<0.0002$), but caused an overall decrease in basal respiration over 72 hours ($P<0.0001$) (**Fig 2.6 D**). Between glucose conditions, metformin-2DG treatment was most effective in a 100mg/dL

glucose condition after 4 and 24 hours at inhibiting basal respiration (P<0.0491, P<0.0001) (**Fig 2.6 C and D**). These data suggest that metformin-2DG treatment is most effective at suppressing the basal respiration of infected cells over time, particularly in a 100mg/dL glucose condition, while having little sustained effects on uninfected cells.

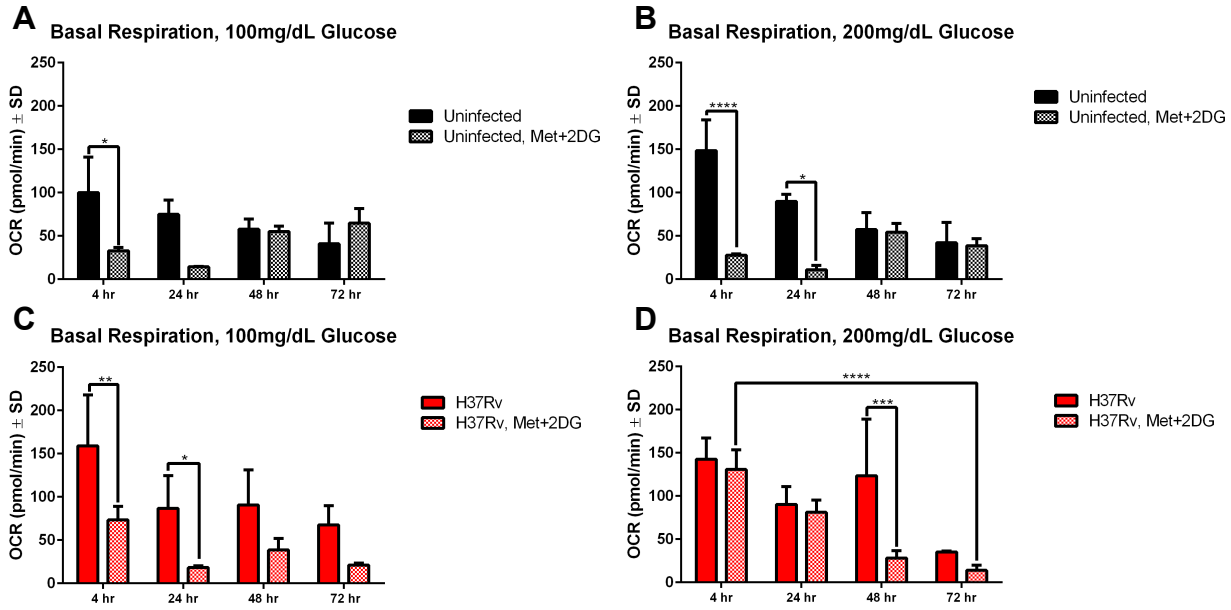

Figure 2.6 Metformin-2DG combined treatment effectively suppresses basal respiration in infected GPBMDMs over time. Basal respiration of uninfected GPBMDMs with and without metformin-2DG combined treatment in (A) 100mg/dL and (B) 200mg/dL glucose conditions. Basal respiration of infected GPBMDMs with and without metformin-2DG combined treatment in (C) 100mg/dL and (D) 200mg/dL glucose conditions. Data is expressed in OCR pmol/min per 65,000 cells ± SD. (A and B) n=6, 2, 3, and 3 in untreated cells, n=3 for all treated cell time points. (C and D) n=8, 4, 3, and 3 in untreated cells and n=3 in all treated cells at specified time points. *=P≤ 0.05, ** =P≤ 0.01, ***=P≤ 0.001, ****=P≤ 0.0001.

Uninfected GPBMDMs under a 100mg/dL glucose condition, metformin-2DG treatment inhibited glycolysis after 4 hours post-treatment (P<0.0333) (**Fig 2.7 A**). Under a 200mg/dL glucose condition, metformin-2DG treatment inhibited glycolysis after 4 and 24 hours post-treatment in uninfected GPBMDMs (P<0.0001, P<0.0068) (**Fig 2.7 B**). Under both glucose conditions, metformin-2DG treatment in uninfected GPBMDMs became ineffective at inhibiting glycolysis after 24 hours (**Fig 2.7 A and B**). Metformin-2DG treatment of infected GPBMDMs inhibited glycolysis starting 24 hours post-treatment in a 100mg/dL glucose condition (P<0.0001) (**Fig 2.7 C**). Significant glycolytic inhibition occurred 48 and 72 hours post treatment

under a 100mg/dL glucose condition (P<0.03, P<0.0145), with an overall inhibition occurring between 4 and 72 hours (P<0.0001) (**Fig 2.7 C**). Under a 200mg/dL glucose condition, glycolytic inhibition occurred 4 and 48 hours post-treatment (P<0.02, P<0.0001), with an overall increase in treatment efficacy over 72 hours (P<0.0025) (**Fig 2.7 D**). Between glucose conditions, metformin-2DG treatment is most effective under a 100mg/dL glucose condition as early as 24 hours post-treatment (P<0.0032), while under a 200mg/L glucose condition, treatment efficacy is delayed 48 hours (P<0.0001) (**Fig 2.7 C and D**). This data indicates that under a 100mg/dL glucose condition, metformin-2DG glycolytic inhibition is most effective due to its rapid and prolonged metabolic suppression. This data reiterates that metformin-2DG treatment becomes ineffective in uninfected GPBMDMs after 24 hours.

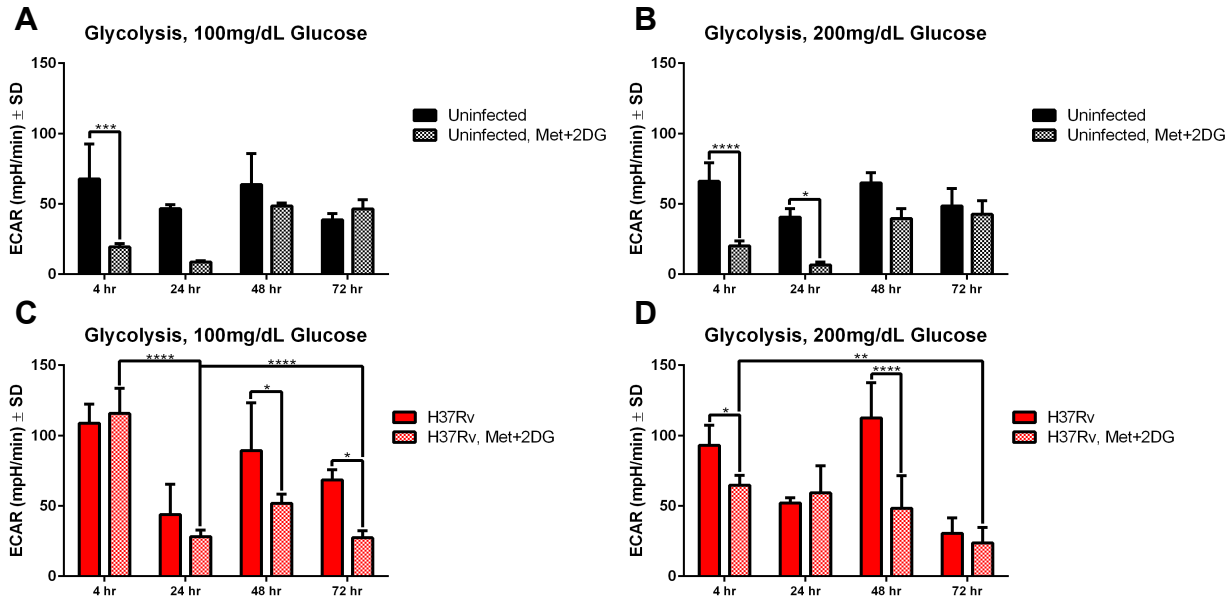

Figure 2.7 Metformin-2DG combined treatment effectively suppresses glycolysis in infected GPBMDMs over time. Glycolysis of uninfected GPBMDMs with and without metformin-2DG combined treatment in (A) 100mg/dL and (B) 200mg/dL glucose conditions. Glycolysis of infected GPBMDMs with and without metformin-2DG combined treatment in (C) 100mg/dL and (D) 200mg/dL glucose conditions. Data is expressed in ECAR mpH/min per 65,000 cells ± SD. (A and B) n=6, 2, 3, and 3 in untreated cells and n=3 for all treated cell time points. (C and D) n=8, 4, 3, and 3 in untreated cells and n=3 for all treated cells at specified time points. *=P≤ 0.05, ** =P≤ 0.01, ***=P≤ 0.001, ****=P≤ 0.0001.

Under both glucose conditions, cellular lactate production increases when singly treated with metformin (P<0.0001), while lactate production is inhibited under 2DG treatment compared

to untreated GPBMDMs (P<0.0001) (**Fig 2.8**). Between 24 and 72 hours metformin-2DG treated GPBMDMs increase lactate production under a 200mg/dL glucose condition (P<0.0087), while lactate production remained inhibited under a 100mg/dL glucose condition (**Fig 2.8**). Statistical significance between the two glucose conditions for metformin-2DG treated cells after 72 hours is P<0.0033. This data confirms that glycolytic inhibition most effectively occurs under a 100mg/dL glucose condition using a combined treatment.

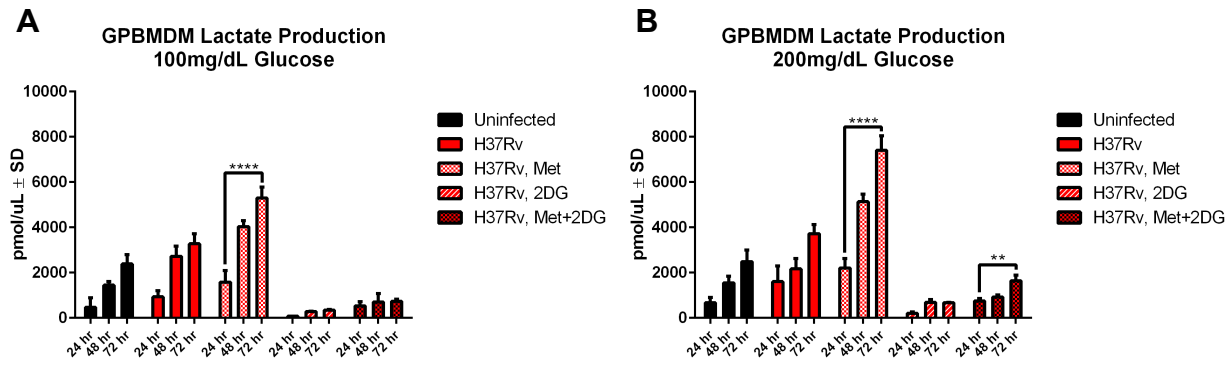

Figure 2.8 Metformin-2DG combined treatment inhibits lactate production more effectively in normal versus high glucose conditions. Lactate production in uninfected (n=3), infected (n=3), and infected-metformin (n=3), 2DG (n=3), and metformin-2DG treated GPBMDMs (n=3) in (A) 100mg/dL and (B) 200mg/dL glucose conditions. Data is expressed in pmol/uL ± SD. *=P≤ 0.05, ** =P≤ 0.01, ***=P≤ 0.001, ****=P≤ 0.0001.

Aim 3: *Determine the effects of metformin, 2-deoxy-glucose, and metformin-2-deoxy-glucose combined therapy on M. tuberculosis and macrophage viability.*

CFUs were plated from infected untreated, metformin treated, 2DG treated, and metformin-2DG treated GPBMDMs. In a 100mg/dL glucose condition, CFUs increased over time in all treatment groups over the first 48 hours, except in metformin-2DG treated GPBMDMs (**Fig 2.9 A**). After 24 hours, the combined treatment decreased CFU counts, restoring them to 4 hour baseline levels (**Fig 2.9 A**). In a 200mg/dL glucose condition, baseline CFU counts began lower than in the 100mg/dL glucose condition (**Fig 2.9 A and B**). However, after 24 hours, CFUs from 2DG treated cells surpassed those observed in the lower glucose condition and outgrew all other sample CFUs by 48 hours (**Fig 2.9 B**). By 72 hours, CFUs from all treatment groups in the 200mg/dL glucose condition were similar to those in the 100mg/dL glucose

condition (**Fig 2.9 A and B**). In the higher glucose condition, the metformin-2DG combined treatment was less effective at inhibiting bacterial growth than in the lower glucose condition. While bacterial growth was suppressed compared to the other treatment groups, it was not inhibited as it was in the lower glucose condition (**Fig 2.9 A and B**). This CFU data suggests that combination treatment enhances GPBMDM bactericidal capacity under a 100mg/dL versus a 200mg/dL glucose condition.

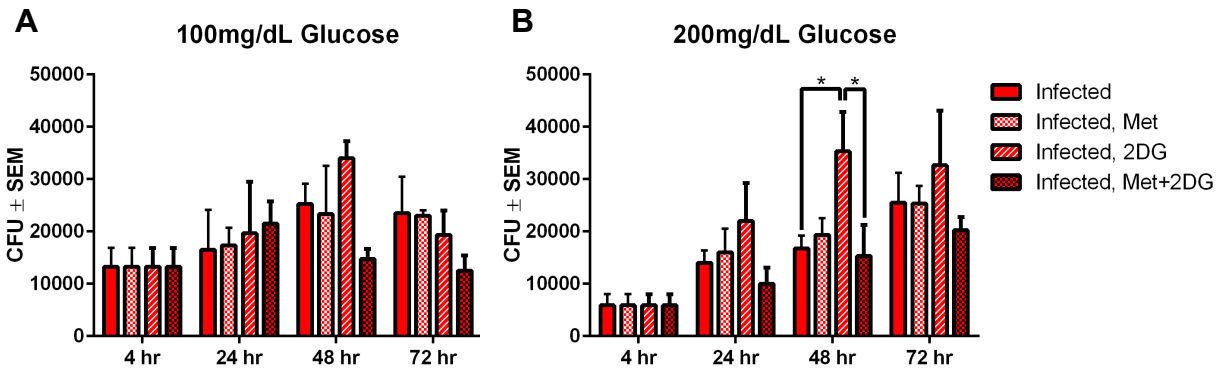

Figure 2.9 Metformin-2DG combined treatment decreases bacterial growth more effectively than metformin or 2DG treatment alone. Mtb CFUs from infected (n=4), and infected-metformin (n=3), 2DG (n=3), and metformin-2DG treated GPBMDMs (n=4) in (A) 100mg/dL and (B) 200mg/dL glucose conditions. Data is expressed in CFU ± SEM. * = P≤0.05.

Under both glucose conditions, 2DG treatment alone significantly decreased cell viability over 72 hours (P<0.0001), while metformin treatment alone had little effect on cell viability compared to untreated GPBMDMs (**Fig 2.10**). Under a 200mg/dL glucose condition, infection alone caused a significant decrease in cell viability from 24 to 72 hours (P<0.0411) (**Fig 2.10 B**). Metformin treatment in combination with 2DG protected GPBMDM cell viability compared to 2DG treatment alone. This data suggests 2DG singly treated GPBMDMs may have a different mechanism of cell death compared to metformin-2DG treated cells, which may be the reason for the notable decrease in bacterial CFUs.

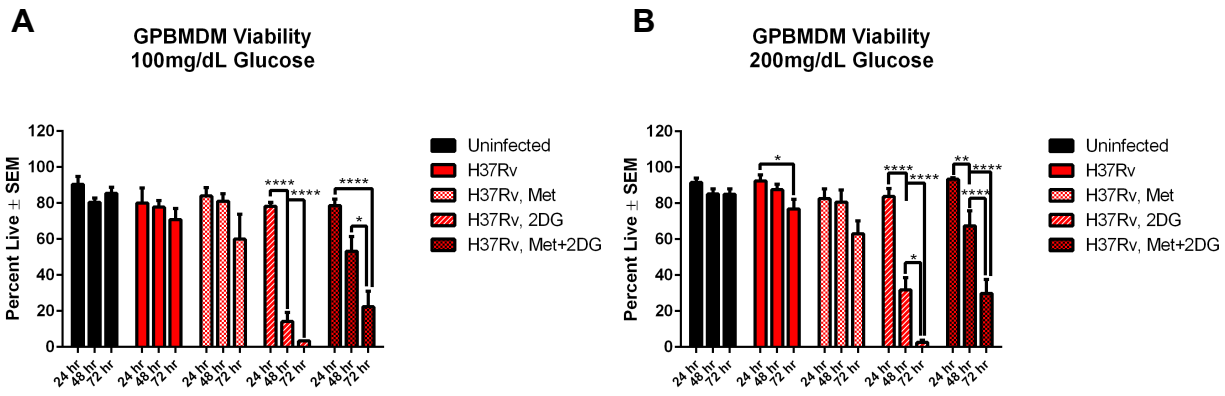

Figure 2.10 Metformin-2DG combined treatment inhibits lactate production more effectively in normal versus high glucose conditions. Cell viability in uninfected, infected, and infected-metformin, 2DG, and metformin-2DG treated GPBMDMs in (A) 100mg/dL and (B) 200mg/dL glucose conditions. Data is expressed in percent live ± standard error of the mean (SEM). (A) n=4, 3, and 7 in uninfected cells, n=7, 7, and 10 in infected cells, n=3, 3, and 3 in infected-metformin and 2DG singly treated cells, n=3, 5, and 6 in infected-metformin-2DG treated cells for each time point. (B) n=5, 3, and 7 in uninfected cells, n=8, 5, and 10 in infected cells, n=3, 3, and 3 in infected-metformin and 2DG singly treated cells, n=6, 5, and 6 in infected-metformin-2DG treated cells for each time point. *=P≤ 0.05, ** =P≤ 0.01, ****=P≤ 0.0001.

To investigate potential mechanisms of cell death, flow cytometric analysis was performed. First we assessed general stages of cell death, which included live, apoptotic, and necrotic according to negative and positive markers for annexin V and SYTOX® AADvanced™ Dead Cell Stain (**Fig 2.11**). After 24 hours both 2DG and metformin-2DG had an increased percent of cells undergoing apoptosis in both 100 and 200mg/dL glucose conditions (**Fig 2.11 A and B**). By 48 hours, the percent of apoptosis was approximately 40 percent greater in 2DG and metformin-2DG treated cells compared to uninfected, infected, and metformin treated cells (**Fig 2.11 C and D**). By 72 hours, apoptosis in 2DG and metformin-2DG treated cells increased by an additional 10 percent compared to all other conditions (**Fig 2.11 E and F**). 24, 48, and 72 hour time points did not reveal significant differences in cell populations between glucose conditions (**Fig 2.11**). While necrotic cell populations were present, the majority was likely lost in the cell staining process.

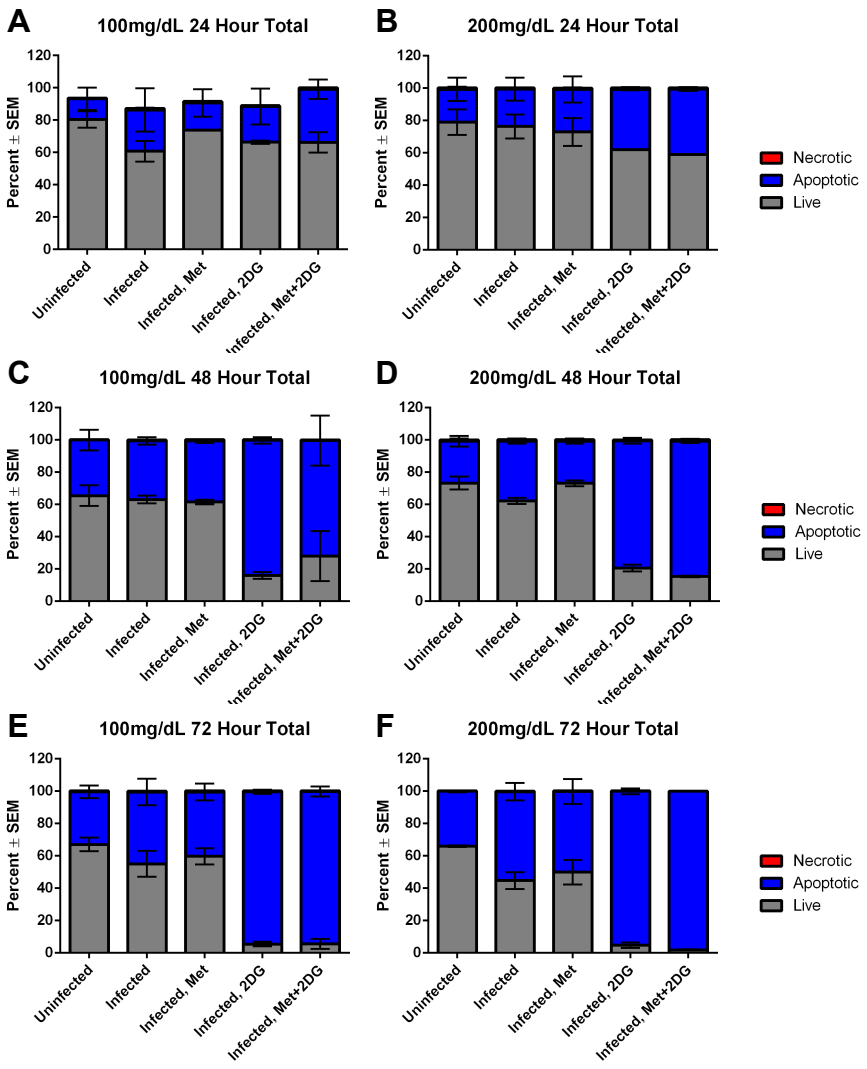

Figure 2.11 2DG and Metformin-2DG combined treatment increase apoptotic cell death in Mtb-infected GPBMDMs after 48 hours. Percent live, apoptotic, and necrotic (A and B) 24 hours, (C and D) 48 hours, and (E and F) 72 hours post-treatment under (A, C, and E) 100 mg/dL and (B, D, and F) 200mg/dL glucose conditions. Data is expressed in percent of total single cells ± SEM. (A-D) n=2, (E-F) n=3.

Next, we discerned the various stages of apoptosis and whether they were caspase 3 and 7 dependent and independent pathways (**Fig 2.12**). At 24 hours, cells in a caspase 3 and 7 independent state predominated 2DG and metformin-2DG treated populations (**Fig 2.12 A and B**). This trend continued through 48 and 72 hours post-treatment (**Fig 2.12 C-F**). There were differences in apoptotic cell stages and caspase dependence between normal and high glucose concentrations at 24 hours, which developed similar profiles by 48 hours (**Fig 2.12 A-D**). At 24

hours, the 100mg/dL glucose condition had an overall lower percent of caspase-dependent apoptosis, while the 200mg/dL glucose condition had more caspase-dependent apoptosis, particularly in the early apoptotic phase (**Fig 2.12 A and B**). Infected cells without treatment had a greater percent of cells in the mid-apoptotic phase at 24 hours in the normal versus high glucose condition (**Fig 2.12 A and B**). Starting at 48 hours, 2DG and metformin-2DG treated cells had 75 percent more mid-phase apoptosis than all other groups (**Fig 2.12 C and D**).

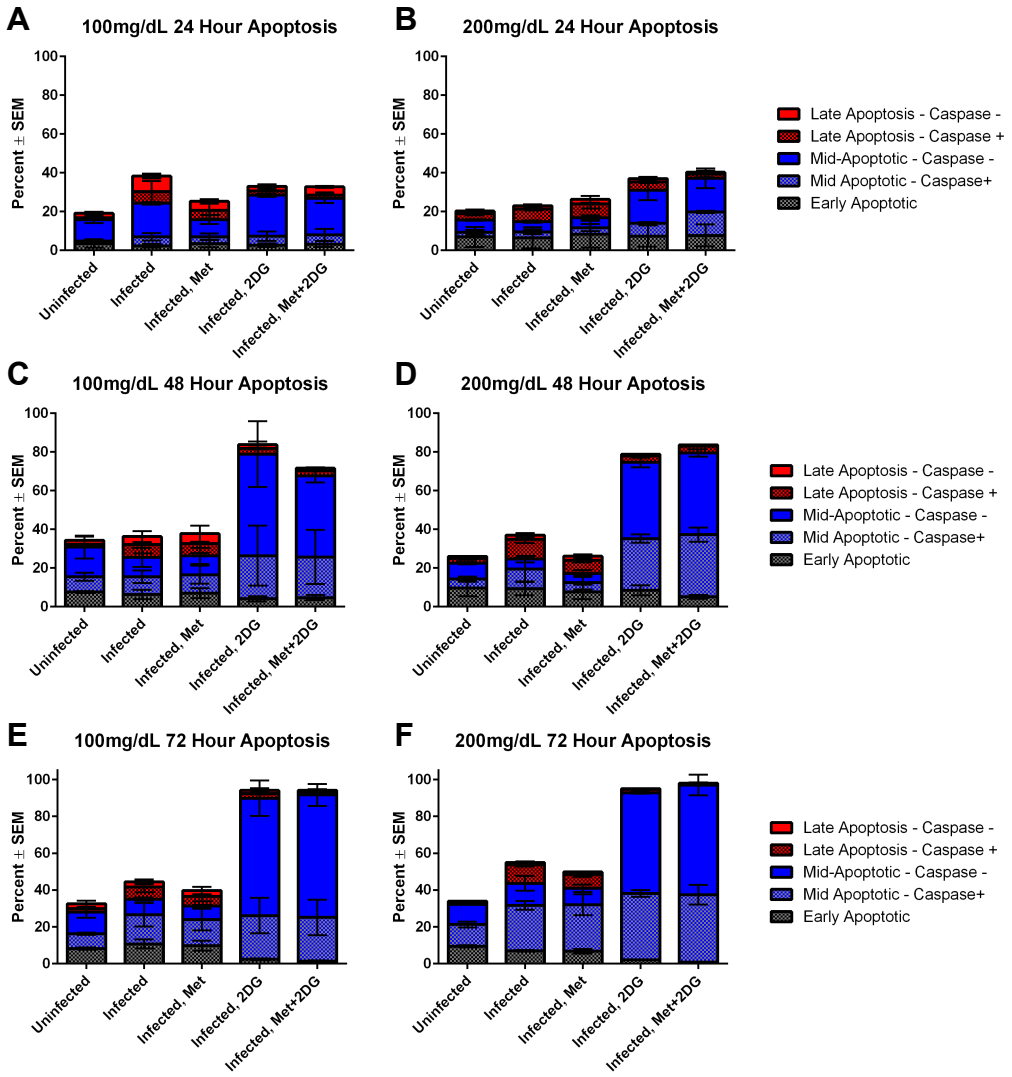

Figure 2.12 2DG and Metformin-2DG treatment increase cells in their mid-apoptotic stage of cell death in Mtb-infected GPBMDMs. Percent of early, mid and late apoptotic cells that are caspase positive or negative (A and B) 24 hours, (C and D) 48 hours, and (E and F) 72 hours post-treatment under (A, C, and E) 100 mg/dL and (B, D, and F) 200mg/dL glucose conditions. Data is expressed in percent of total single cells ± SEM. (A-D) n=2, (E-F) n=3.

Autophagy was assessed with the autophagosome marker monodansylcadaverine in live, apoptotic, and necrotic cell populations within each condition over time (**Fig 2.13**). At 24 hours, similar profiles were noted between glucose conditions and among treatment groups (**Fig 2.13 A and B**). At 48 and 72 hours, the normal glucose condition had 25 percent less autophagosome formation than the high glucose condition, with the most extensive inhibition with 2DG and metformin-2DG treatments (**Fig 2.13 C-F**). However, 2DG treated cells had approximately 10 percent more autophagy than metformin-2DG treated cells (**Fig 2.13 C and D**). Collectively this data suggests that 2DG and metformin-2DG treatments generate similar mechanisms of cell death and similar autophagy trends, but demonstrate opposite trends in bacterial CFUs. This suggests that bacterial death associated with metformin-2DG treatment is not dependent on apoptosis or autophagy.

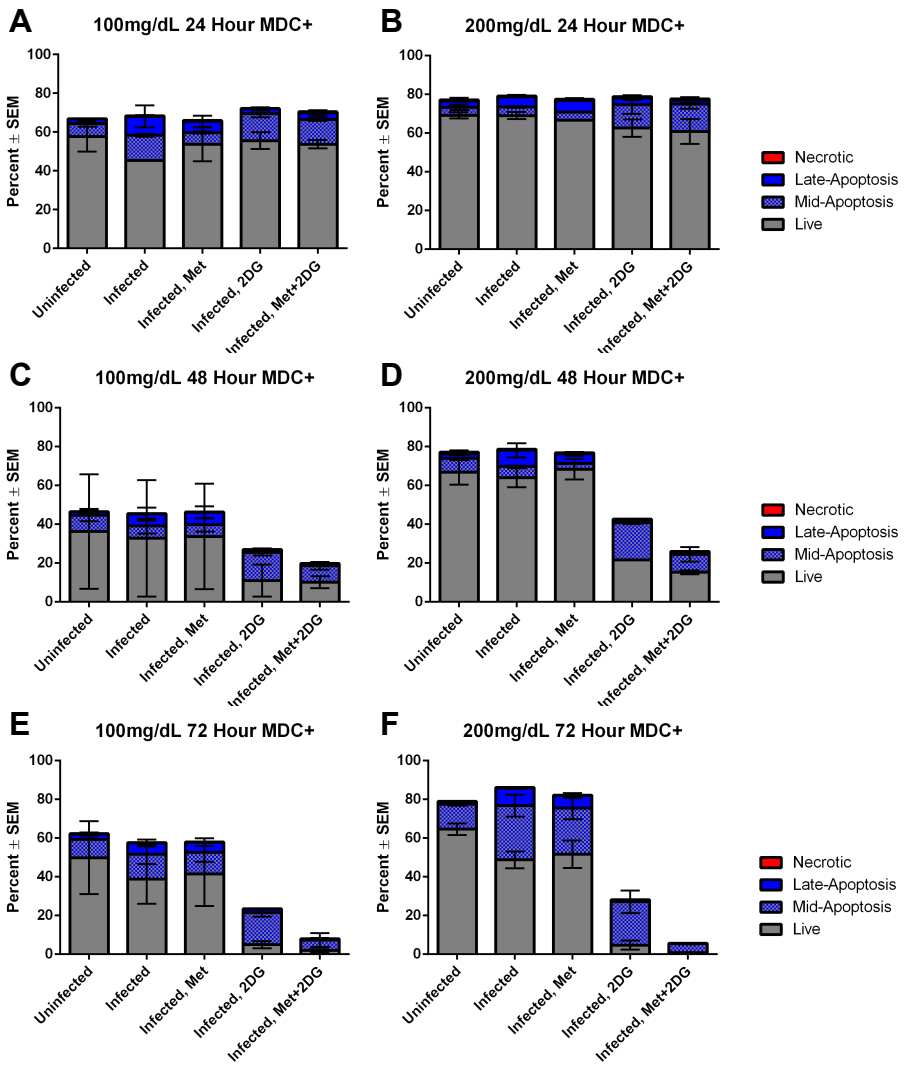

Figure 2.13 2DG and Metformin-2DG treatment inhibited baseline levels of autophagy in Mtb-infected GPBMDMs. Percent of live, mid and late apoptotic, and necrotic cells (A and B) 24 hours, (C and D) 48 hours, and (E and F) 72 hours post-treatment under (A, C, and E) 100 mg/dL and (B, D, and F) 200mg/dL glucose conditions. Data is expressed in percent of total single cells ± SEM. (A-D) n=2 and (E-F) n=3.

DISCUSSION

With MDR TB cases on the rise and lags in antimicrobial drug development, it is imperative to explore alternative methods of treatment such as host-directed adjunct therapies. One therapeutic opportunity is to reduce chronic non-diabetic hyperglycemia associated with Mtb infection. Metformin, an anti-diabetic drug, acts on both cellular and systemic levels by stimulating glycolysis within the liver and other cell types via partial inhibition of oxidative phosphorylation, subsequently decreasing blood glucose levels. Treatment of infected M1 macrophages with metformin increases cellular metabolic stress by increasing glycolysis in already glycolytic cells. The addition of 2DG, a glycolytic inhibitor, in combination with metformin further exacerbates this metabolic stress, which can favorably induce mitochondrial-driven apoptotic cell death. This mechanism of cell death can increase Mtb-clearance and antigen presentation, enabling the activation of adaptive immune responses. From this information we hypothesized that bacterial survival is aided by glycolysis-dependent macrophages, which can be targeted using a combination of metformin and 2DG to strengthen host immune responses.

The first aim was to determine the effect of normal versus high glucose concentrations on glucose metabolism in activated macrophages. Consistent with other studies, we confirmed that activated and Mtb-infected macrophages rely more on glycolysis than uninfected macrophages[17,18,23,26,65]. In addition to increased glycolysis, we observed that Mtb-infected macrophages also increase their basal respiration, both peaking after 48 hours. This simultaneous increase likely indicates pro-inflammatory, bactericidal macrophage activation where glycolysis is upregulated to generate ATP and oxygen consumption increases for mitochondrial ROS production[19]. However, we also observed that metabolic responses to infection are impaired under a high glucose environment. Upon infection, basal respiration did not increase from a quiescent macrophage state and glycolytic responses were delayed. This aligns with past studies concluding that cells under a high glucose condition have an impaired

pro-inflammatory responses to infection, such as glycolytic upregulation and mitochondrial ROS production[35-37]. Macrophages infected under a high glucose condition also demonstrated lower initial bacterial CFUs compared to macrophages infected under a normal glucose environment, which may confirm previous studies suggesting impaired phagocytic capabilities under hyperglycemia[35]. Data gathered under this aim suggests that a high glucose environment impairs macrophage responses to infection by generating insufficient metabolic shifts to perform effective bactericidal functions.

Next, we determined the level of inhibition of metformin, 2DG, and combined metformin-2DG treatment on the altered metabolism of Mtb-infected macrophages. Aligning with their proposed mechanisms of action, metformin treatment increased while 2DG treatment inhibited glycolytic activity[64]. In combination, metformin-2DG treatment partially inhibited glycolysis compared to untreated cells, indicating that metformin moderates the inhibitory mechanism of 2DG. This is likely due to the increased glycolytic activity by metformin offsetting the competitive inhibition of 2DG on glucose. Over 72 hours, metformin-2DG treatment provided sustained inhibition of basal respiration and glycolytic activity in Mtb-infected macrophages. The suppression of both rates may inhibit both mitochondrial ROS production and glycolytic dependence on ATP generation, rendering the cell incapable of performing its normal physiologic responses to infection, while simultaneously placing metabolic stress on the cell. However in uninfected macrophages, metformin-2DG treatment became ineffective after 48 hours, restoring both respiratory and glycolytic rates to an uninfected, untreated state. This indicates that metformin-2DG treatment is most effective at targeting cells with an upregulated, altered metabolism, while maintaining the metabolic stability in those unaffected. When assessed under a high glucose condition, inhibition of basal respiration and glycolysis by metformin-2DG treatment were delayed in Mtb-infected macrophages demonstrating that metformin-2DG treatment is most effective in activated cells that are highly dependent on glycolysis for energy production. These observations suggest that metformin-2DG treatment

may be an ideal therapy for predominantly targeting the metabolic activity of Mtb-infected versus uninfected macrophages.

The final aim was to determine the effects of metformin, 2DG and metformin-2DG treatment on Mtb and macrophage viability. As confirmed by Gleeson et al, 2DG treatment increased bacterial viability, while metformin-2DG treatment decreased bacterial viability over time[65]. This data suggests that the cell death associated with metformin-2DG treatment can clear bacterial infections, whereas macrophage death by 2DG treatment alone is ineffective, enabling bacterial survival. When assessed via Trypan blue dye exclusion assay, macrophage viability was not dependent on glucose condition, meaning that all treatments produced similar responses to cell death regardless of normal or high glucose conditions. While metformin had little effect on cell viability, 2DG potentiated cell death over 72 hours. However, in combination, metformin was protective against 2DG-related cell death. To contrast these results, flow cytometry revealed similar cell death trends and populations between 2DG and metformin-2DG treatments. These groups had increased apoptotic cell death and inhibited autophagy over time. A potential explanation for this unexpected result is that the inclusion of metformin with 2DG may activate other survival or death pathways, including an alternate method of apoptosis. While the exact mechanism has yet to be elucidated, it is possible that the metformin-2DG treatment may be enabling antigen presentation through the observed decrease in bacterial survival.

While glucose condition had little effect on macrophage viability, it did make a difference in bacterial survival and replication. Initially, bacterial CFUs were lower under the high glucose condition compared to the normal glucose condition. However, over time bacterial growth under the high glucose environment surpassed those under the normal glucose condition. This suggests that impaired macrophage responses to infection due to high glucose concentrations favors bacterial survival. Despite increasing bacterial survival, metformin-2DG treatment was capable of curtailing bacterial growth over the 72-hour time span demonstrating that even under

high glucose conditions, metformin-2DG treatment can restore macrophage responses to infection.

Collectively, we can conclude that bacterial survival is not dependent on macrophage glycolysis as demonstrated by the increase in CFUs in 2DG-only treated cells. However, the use of both metformin and 2DG in combination was effective under both normal and high glucose conditions at controlling bacterial growth. Additionally, metformin-2DG treatment targets cells with an upregulated glycolytic glucose metabolism, and increasing apoptotic death of these cells, thus generating opportunities for antigen presentation to stimulate an adaptive immune response. Overall, this combination therapy shows promise as a potential adjunct host-directed therapy to be tested in *in vivo* models.

Limitations

However, there are some limitations to consider. The first limitation is related to the treatment. While the biologically relevant metformin dose is 12uM, our data revealed the optimal *in vitro* dose in combination with 2DG to be 600uM after 24 hours. This dose is 50 times higher than what is achievable *in vivo*, but is still less than concentrations used by other published studies (1 or 2mM). Another consideration is that the treatment was added 4 hours post-infection, thus the observed treatment outcomes may be different if added after longer periods of infection. A final consideration related to treatment is the addition of the compounds. In this study, they were simultaneously added to cell culture, but treatment outcomes may be enhanced or minimized according to how and when each compound is added.

The second set of limitations is associated with the use of an *in vitro* versus *in vivo* model. Under an *in vitro* system, there is not a continuous influx and efflux of nutrients, byproducts, and compounds as there would be *in vivo*. Therefore, we do not know how metformin and 2DG function under dynamic conditions such as contact time and accumulation among infected cells. We also do not know if the cell death trends noted *in vitro* will be reflected *in vivo*. A final and important consideration is the absence of a complete immune response

within an *in vitro* model. If the combination of metformin and 2DG potentiates antigen presentation via apoptosis, we do not know if bacterial clearance will be augmented via the initiation of adaptive immune responses. Despite these limitations, this study provides sufficient evidence for further investigation of metformin-2DG treatment *in vivo*.

PROJECT SUMMARY AND FUTURE DIRECTIONS

The purpose of this project was to determine if a combination treatment of metformin and 2-deoxyglucose (2DG) would aid in bacterial clearance through host-directed apoptotic cell death. To test this hypothesis, we determined the metabolic status of uninfected compared to *Mycobacterium tuberculosis* (Mtb) infected macrophages under physiologic normal (100mg/dL) and high glucose (200mg/dL) conditions as are present under acute and chronic TB infection, respectively. We measured the basal respiration and glycolytic activity of these macrophages under these various conditions over 72 hours. It was observed that infected macrophages have a sustained increase in both basal respiration and glycolytic rates over 72 hours, but that high glucose conditions impaired early glycolytic and respiratory responses to infection.

Next we determined the impact metformin, 2DG, and metformin-2DG combined treatments had on Mtb and macrophage metabolism. The three treatments had no effect on Mtb growth or metabolism, but had notable effects on macrophage metabolism. In Mtb-infected macrophages, metformin treatment alone decreased basal respiration, but increased glycolysis in a dose-dependent manner at both 4 and 24 hours post treatment. 2DG showed little effect on basal respiration, but effectively inhibited glycolytic activity after just 4 hours of treatment. Both treatment outcomes are consistent with each compound's mechanism of action. Combined, metformin-2DG treatment significantly inhibited basal respiration after 4 and 24 hours post-treatment, and inhibited glycolytic activity as efficiently as 2DG treatment alone. This suggests that both compounds work with equal or greater efficacy in combination. Metformin-2DG treatment in Mtb-infected macrophages sustained basal respiration and glycolytic inhibition over 72 hours, but became ineffective in uninfected macrophages after 24 hours, suggesting a targeted treatment for pro-inflammatory cells with increased glycolytic metabolism. The combined treatment worked best under a normal glucose condition, demonstrating that the

blood glucose lowering impact of metformin would potentiate its cellular effects in conjunction with 2DG.

A final assessment was performed on macrophage and Mtb viability after treatment with metformin, 2DG, or metformin-2DG under both glucose conditions. Metformin did not significantly impact cell viability, while 2DG and metformin-2DG treatments caused 90% and 30-35% losses in cell viability, respectively. Discriminating between methods of cell death, 2DG metformin-2DG treatment revealed similar levels of apoptosis and inhibition of autophagy. This suggests that decreased Mtb viability in metformin-2DG treated cells is not associated with apoptosis or autophagy. However, these results also suggest that the combined metformin-2DG treatment may be effective at increasing antigen presentation if presented with adaptive immune cells.

Future investigation on this topic should include varying the administration of metformin-2DG combination treatment *in vitro* and attempting this treatment *in vivo*. An additional *in vitro* study should be performed to determine how the order and timing of treatment affects treatment outcomes. The addition of either metformin and/or 2DG first may either enhance or decrease treatment efficacy. Also, the addition of these compounds after 24, 48, or 72 hours of infection may also affect macrophage bacterial clearance. Another *in vitro* study should determine if cell-mediated immunity is increased by metformin-2DG treatment. To test this hypothesis, lymphocytes would be added to Mtb-infected macrophages and treated with metformin-2DG to assess lymphocyte activation, proliferation and metabolic responses.

In vivo, metformin-2DG treatment should be assessed under both acute and chronic infection as well as in combination with first-line TB antimicrobial drugs, including rifampicin, pyrazinamide, and isoniazid. First, the effects of order, timing, and duration of treatment would need to be determined in terms of Mtb clearance and animal health status. Once a treatment regimen is generated, assessment of metformin-2DG treatment on antimicrobial drug efficacy,

Mtb clearance, and cell-mediated immune responses would determine the viability of these compounds as a host-directed therapy.

REFERENCES

1 2015 Global Tuberculosis Report. (Geneva, Switzerland, 2015).

2 Zumla, A., Raviglione, M., Hafner, R. & von Reyn, C. F. Tuberculosis. *The New England journal of medicine* **368**, 745-755, doi:10.1056/NEJMra1200894 (2013).

3 Hershkovitz, I. *et al.* Detection and molecular characterization of 9,000-year-old Mycobacterium tuberculosis from a Neolithic settlement in the Eastern Mediterranean. *PloS one* **3**, e3426, doi:10.1371/journal.pone.0003426 (2008).

4 Dheda, K., Barry, C. E., 3rd & Maartens, G. Tuberculosis. *Lancet* **387**, 1211-1226, doi:10.1016/S0140-6736(15)00151-8 (2016).

5 Frieden, T. R., Sterling, T. R., Munsiff, S. S., Watt, C. J. & Dye, C. Tuberculosis. *Lancet* **362**, 887-899, doi:10.1016/S0140-6736(03)14333-4 (2003).

6 Ehrt, S. & Rhee, K. Mycobacterium tuberculosis metabolism and host interaction: mysteries and paradoxes. *Curr Top Microbiol Immunol* **374**, 163-188, doi:10.1007/82_2012_299 (2013).

7 Guirado, E., Schlesinger, L. S. & Kaplan, G. Macrophages in tuberculosis: friend or foe. *Semin Immunopathol* **35**, 563-583, doi:10.1007/s00281-013-0388-2 (2013).

8 Ramakrishnan, L. Revisiting the role of the granuloma in tuberculosis. *Nature reviews. Immunology* **12**, 352-366, doi:10.1038/nri3211 (2012).

9 Vergne, I. *et al.* Mycobacterium tuberculosis phagosome maturation arrest: mycobacterial phosphatidylinositol analog phosphatidylinositol mannoside stimulates early endosomal fusion. *Molecular biology of the cell* **15**, 751-760, doi:10.1091/mbc.E03-05-0307 (2004).

10 Hmama, Z., Pena-Diaz, S., Joseph, S. & Av-Gay, Y. Immunoevasion and immunosuppression of the macrophage by Mycobacterium tuberculosis. *Immunological reviews* **264**, 220-232, doi:10.1111/imr.12268 (2015).

11 Philips, J. A. & Ernst, J. D. Tuberculosis pathogenesis and immunity. *Annual review of pathology* **7**, 353-384, doi:10.1146/annurev-pathol-011811-132458 (2012).

12 Benoit, M., Desnues, B. & Mege, J. L. Macrophage polarization in bacterial infections. *Journal of immunology* **181**, 3733-3739 (2008).

13 Sica, A. & Mantovani, A. Macrophage plasticity and polarization: in vivo veritas. *The Journal of clinical investigation* **122**, 787-795, doi:10.1172/JCI59643 (2012).

14 Galvan-Pena, S. & O'Neill, L. A. Metabolic reprograming in macrophage polarization. *Front Immunol* **5**, 420, doi:10.3389/fimmu.2014.00420 (2014).

15 Sica, A., Erreni, M., Allavena, P. & Porta, C. Macrophage polarization in pathology. *Cell Mol Life Sci* **72**, 4111-4126, doi:10.1007/s00018-015-1995-y (2015).

16 Palsson-McDermott, E. M. & O'Neill, L. A. The Warburg effect then and now: from cancer to inflammatory diseases. *Bioessays* **35**, 965-973, doi:10.1002/bies.201300084 (2013).

17 Marino, S. *et al.* Macrophage polarization drives granuloma outcome during Mycobacterium tuberculosis infection. *Infection and immunity* **83**, 324-338, doi:10.1128/IAI.02494-14 (2015).

18 Qualls, J. E. & Murray, P. J. Immunometabolism within the tuberculosis granuloma: amino acids, hypoxia, and cellular respiration. *Semin Immunopathol* **38**, 139-152, doi:10.1007/s00281-015-0534-0 (2016).

19 Ganeshan, K. & Chawla, A. Metabolic regulation of immune responses. *Annu Rev Immunol* **32**, 609-634, doi:10.1146/annurev-immunol-032713-120236 (2014).

20 Vazquez, A., Liu, J., Zhou, Y. & Oltvai, Z. N. Catabolic efficiency of aerobic glycolysis: the Warburg effect revisited. *BMC systems biology* **4**, 58, doi:10.1186/1752-0509-4-58 (2010).
21 Ghesquiere, B., Wong, B. W., Kuchnio, A. & Carmeliet, P. Metabolism of stromal and immune cells in health and disease. *Nature* **511**, 167-176, doi:10.1038/nature13312 (2014).
22 Weinberg, S. E., Sena, L. A. & Chandel, N. S. Mitochondria in the regulation of innate and adaptive immunity. *Immunity* **42**, 406-417, doi:10.1016/j.immuni.2015.02.002 (2015).
23 Lin, P. L. *et al.* Radiologic responses in cynomolgous macaques for assessing tuberculosis chemotherapy regimens. *Antimicrobial agents and chemotherapy*, doi:10.1128/AAC.00277-13 (2013).
24 Chang, J. M. *et al.* False positive and false negative FDG-PET scans in various thoracic diseases. *Korean J Radiol* **7**, 57-69 (2006).
25 Tavakoli, S., Zamora, D., Ullevig, S. & Asmis, R. Bioenergetic profiles diverge during macrophage polarization: implications for the interpretation of 18F-FDG PET imaging of atherosclerosis. *J Nucl Med* **54**, 1661-1667, doi:10.2967/jnumed.112.119099 (2013).
26 Somashekar, B. S. *et al.* Metabolic profiling of lung granuloma in Mycobacterium tuberculosis infected guinea pigs: ex vivo 1H magic angle spinning NMR studies. *J Proteome Res* **10**, 4186-4195, doi:10.1021/pr2003352 (2011).
27 Bell, L., Bhat, V., George, G., Awotedu, A. A. & Gqaza, B. Sluggish glucose tolerance in tuberculosis patients. *S Afr Med J* **97**, 374-377 (2007).
28 Jorgensen, M. E. & Faurholt-Jepsen, D. Is there an effect of glucose lowering treatment on incidence and prognosis of tuberculosis? A systematic review. *Curr Diab Rep* **14**, 505, doi:10.1007/s11892-014-0505-1 (2014).
29 Boillat-Blanco, N. *et al.* Transient Hyperglycemia in Patients With Tuberculosis in Tanzania: Implications for Diabetes Screening Algorithms. *The Journal of infectious diseases* **213**, 1163-1172, doi:10.1093/infdis/jiv568 (2016).
30 Preiser, J. C., Ichai, C., Orban, J. C. & Groeneveld, A. B. Metabolic response to the stress of critical illness. *Br J Anaesth* **113**, 945-954, doi:10.1093/bja/aeu187 (2014).
31 Basoglu, O. K., Bacakoglu, F., Cok, G., Sayiner, A. & Ates, M. The oral glucose tolerance test in patients with respiratory infections. *Monaldi Arch Chest Dis* **54**, 307-310 (1999).
32 Oluboyo, P. O. & Erasmus, R. T. The significance of glucose intolerance in pulmonary tuberculosis. *Tubercle* **71**, 135-138 (1990).
33 Gulbas, Z., Erdogan, Y. & Balci, S. Impaired glucose tolerance in pulmonary tuberculosis. *Eur J Respir Dis* **71**, 345-347 (1987).
34 Podell, B. K. *et al.* Non-diabetic hyperglycemia exacerbates disease severity in Mycobacterium tuberculosis infected guinea pigs. *PloS one* **7**, e46824, doi:10.1371/journal.pone.0046824 (2012).
35 Restrepo, B. I., Twahirwa, M., Rahbar, M. H. & Schlesinger, L. S. Phagocytosis via complement or Fc-gamma receptors is compromised in monocytes from type 2 diabetes patients with chronic hyperglycemia. *PloS one* **9**, e92977, doi:10.1371/journal.pone.0092977 (2014).
36 Lachmandas, E. *et al.* The effect of hyperglycaemia on in vitro cytokine production and macrophage infection with Mycobacterium tuberculosis. *PloS one* **10**, e0117941, doi:10.1371/journal.pone.0117941 (2015).
37 Xiu, F., Stanojcic, M., Diao, L. & Jeschke, M. G. Stress hyperglycemia, insulin treatment, and innate immune cells. *Int J Endocrinol* **2014**, 486403, doi:10.1155/2014/486403 (2014).

38 Nishizawa, T. & Bornfeldt, K. E. Diabetic vascular disease and the potential role of macrophage glucose metabolism. *Ann Med* **44**, 555-563, doi:10.3109/07853890.2011.585346 (2012).
39 Hodgson, K. *et al.* Immunological mechanisms contributing to the double burden of diabetes and intracellular bacterial infections. *Immunology* **144**, 171-185, doi:10.1111/imm.12394 (2015).
40 Lee, J., Hartman, M. & Kornfeld, H. Macrophage apoptosis in tuberculosis. *Yonsei Med J* **50**, 1-11, doi:10.3349/ymj.2009.50.1.1 (2009).
41 Green, D. R. & Llambi, F. Cell Death Signaling. *Cold Spring Harb Perspect Biol* **7**, doi:10.1101/cshperspect.a006080 (2015).
42 Moraco, A. H. & Kornfeld, H. Cell death and autophagy in tuberculosis. *Semin Immunol* **26**, 497-511, doi:10.1016/j.smim.2014.10.001 (2014).
43 Green, D. R., Galluzzi, L. & Kroemer, G. Cell biology. Metabolic control of cell death. *Science* **345**, 1250256, doi:10.1126/science.1250256 (2014).
44 Altman, B. J. & Rathmell, J. C. Metabolic stress in autophagy and cell death pathways. *Cold Spring Harb Perspect Biol* **4**, a008763, doi:10.1101/cshperspect.a008763 (2012).
45 MacFarlane, M., Robinson, G. L. & Cain, K. Glucose--a sweet way to die: metabolic switching modulates tumor cell death. *Cell Cycle* **11**, 3919-3925, doi:10.4161/cc.21804 (2012).
46 Lindqvist, L. M., Simon, A. K. & Baehrecke, E. H. Current questions and possible controversies in autophagy. *Cell Death Discov* **1**, doi:10.1038/cddiscovery.2015.36 (2015).
47 Gutierrez, M. G. *et al.* Autophagy is a defense mechanism inhibiting BCG and Mycobacterium tuberculosis survival in infected macrophages. *Cell* **119**, 753-766, doi:10.1016/j.cell.2004.11.038 (2004).
48 Behar, S. M. & Baehrecke, E. H. Tuberculosis: Autophagy is not the answer. *Nature* **528**, 482-483, doi:10.1038/nature16324 (2015).
49 Kimmey, J. M. *et al.* Unique role for ATG5 in neutrophil-mediated immunopathology during M. tuberculosis infection. *Nature* **528**, 565-569, doi:10.1038/nature16451 (2015).
50 Derrick, S. C. & Morris, S. L. The ESAT6 protein of Mycobacterium tuberculosis induces apoptosis of macrophages by activating caspase expression. *Cellular microbiology* **9**, 1547-1555, doi:10.1111/j.1462-5822.2007.00892.x (2007).
51 Santucci, M. B. *et al.* Mycobacterium tuberculosis-induced apoptosis in monocytes/macrophages: early membrane modifications and intracellular mycobacterial viability. *The Journal of infectious diseases* **181**, 1506-1509, doi:10.1086/315371 (2000).
52 Davis, J. M. & Ramakrishnan, L. The role of the granuloma in expansion and dissemination of early tuberculous infection. *Cell* **136**, 37-49, doi:10.1016/j.cell.2008.11.014 (2009).
53 Pernicova, I. & Korbonits, M. Metformin--mode of action and clinical implications for diabetes and cancer. *Nat Rev Endocrinol* **10**, 143-156, doi:10.1038/nrendo.2013.256 (2014).
54 Singhal, A. *et al.* Metformin as adjunct antituberculosis therapy. *Sci Transl Med* **6**, 263ra159, doi:10.1126/scitranslmed.3009885 (2014).
55 Ben Sahra, I., Le Marchand-Brustel, Y., Tanti, J. F. & Bost, F. Metformin in cancer therapy: a new perspective for an old antidiabetic drug? *Molecular cancer therapeutics* **9**, 1092-1099, doi:10.1158/1535-7163.MCT-09-1186 (2010).
56 Pryor, R. & Cabreiro, F. Repurposing metformin: an old drug with new tricks in its binding pockets. *The Biochemical journal* **471**, 307-322, doi:10.1042/BJ20150497 (2015).
57 Birsoy, K. *et al.* Metabolic determinants of cancer cell sensitivity to glucose limitation and biguanides. *Nature* **508**, 108-112, doi:10.1038/nature13110 (2014).

58 Menendez, J. A. *et al.* Metformin is synthetically lethal with glucose withdrawal in cancer cells. *Cell Cycle* **11**, 2782-2792, doi:10.4161/cc.20948 (2012).
59 Matsuo, J. *et al.* Hyperactivation of 4E-binding protein 1 as a mediator of biguanide-induced cytotoxicity during glucose deprivation. *Molecular cancer therapeutics* **11**, 1082-1091, doi:10.1158/1535-7163.MCT-11-0871 (2012).
60 Zhuang, Y., Chan, D. K., Haugrud, A. B. & Miskimins, W. K. Mechanisms by which low glucose enhances the cytotoxicity of metformin to cancer cells both in vitro and in vivo. *PloS one* **9**, e108444, doi:10.1371/journal.pone.0108444 (2014).
61 Bikas, A. *et al.* Glucose-deprivation increases thyroid cancer cells sensitivity to metformin. *Endocr Relat Cancer* **22**, 919-932, doi:10.1530/ERC-15-0402 (2015).
62 Park, D. B. Metformin Promotes Apoptosis but Suppresses Autophagy in Glucose-Deprived H4IIE Hepatocellular Carcinoma Cells. *Diabetes Metab J* **39**, 518-527, doi:10.4093/dmj.2015.39.6.518 (2015).
63 Cheong, J. H. *et al.* Dual inhibition of tumor energy pathway by 2-deoxyglucose and metformin is effective against a broad spectrum of preclinical cancer models. *Molecular cancer therapeutics* **10**, 2350-2362, doi:10.1158/1535-7163.MCT-11-0497 (2011).
64 Vincent, E. E. *et al.* Differential effects of AMPK agonists on cell growth and metabolism. *Oncogene* **34**, 3627-3639, doi:10.1038/onc.2014.301 (2015).
65 Gleeson, L. E. *et al.* Cutting Edge: Mycobacterium tuberculosis Induces Aerobic Glycolysis in Human Alveolar Macrophages That Is Required for Control of Intracellular Bacillary Replication. *Journal of immunology* **196**, 2444-2449, doi:10.4049/jimmunol.1501612 (2016).
66 Aykin-Burns, N., Ahmad, I. M., Zhu, Y., Oberley, L. W. & Spitz, D. R. Increased levels of superoxide and H2O2 mediate the differential susceptibility of cancer cells versus normal cells to glucose deprivation. *The Biochemical journal* **418**, 29-37, doi:10.1042/BJ20081258 (2009).
67 Jiang, W., Zhu, Z. & Thompson, H. J. Modulation of the activities of AMP-activated protein kinase, protein kinase B, and mammalian target of rapamycin by limiting energy availability with 2-deoxyglucose. *Molecular carcinogenesis* **47**, 616-628, doi:10.1002/mc.20425 (2008).
68 Matsuda, F., Fujii, J. & Yoshida, S. Autophagy induced by 2-deoxy-D-glucose suppresses intracellular multiplication of Legionella pneumophila in A/J mouse macrophages. *Autophagy* **5**, 484-493 (2009).
69 Wang, Q., Liang, B., Shirwany, N. A. & Zou, M. H. 2-Deoxy-D-glucose treatment of endothelial cells induces autophagy by reactive oxygen species-mediated activation of the AMP-activated protein kinase. *PloS one* **6**, e17234, doi:10.1371/journal.pone.0017234 (2011).
70 Zhou, G. *et al.* Role of AMP-activated protein kinase in mechanism of metformin action. *The Journal of clinical investigation* **108**, 1167-1174, doi:10.1172/JCI13505 (2001).
71 Ben Sahra, I. *et al.* Targeting cancer cell metabolism: the combination of metformin and 2-deoxyglucose induces p53-dependent apoptosis in prostate cancer cells. *Cancer research* **70**, 2465-2475, doi:10.1158/0008-5472.CAN-09-2782 (2010).
72 Xue, C. *et al.* Targeting P-glycoprotein expression and cancer cell energy metabolism: combination of metformin and 2-deoxyglucose reverses the multidrug resistance of K562/Dox cells to doxorubicin. *Tumour Biol*, doi:10.1007/s13277-015-4478-8 (2016).
73 Padilla-Carlin, D. J., McMurray, D. N. & Hickey, A. J. The guinea pig as a model of infectious diseases. *Comp Med* **58**, 324-340 (2008).
74 McMurray, D. N. Disease model: pulmonary tuberculosis. *Trends Mol Med* **7**, 135-137 (2001).
75 Orme, I. M. & Basaraba, R. J. The formation of the granuloma in tuberculosis infection. *Semin Immunol* **26**, 601-609, doi:10.1016/j.smim.2014.09.009 (2014).

76 Graham, G. G. *et al.* Clinical pharmacokinetics of metformin. *Clin Pharmacokinet* **50**, 81-98, doi:10.2165/11534750-000000000-00000 (2011).
77 Gounder, M. K. *et al.* A validated bioanalytical HPLC method for pharmacokinetic evaluation of 2-deoxyglucose in human plasma. *Biomed Chromatogr* **26**, 650-654, doi:10.1002/bmc.1710 (2012).